



A 3,000-yr lacustrine record of climate and environmental change and their influence on aquatic communities from Andean Puna lakes

Adriana Aránguiz-Acuña^{1,2}, Daniel Pérez^{1,2}, Catalina Aranda^{1,2}, Antonio Maldonado^{2,3}, Joseline Tapia^{2,4}, Héctor Pizarro⁴, Pablo Pérez-Portilla^{1,2,4}, Oliver Meseguer-Ruiz^{2,5}

5

¹Laboratorio de Ecología Acuática, Departamento de Química, Universidad de Tarapacá. Arica, Chile

²Millennium Nucleus of Andean Peatlands, AndesPeat. Arica, Chile.

³Centro de Estudios Avanzados en Zonas Áridas (CEAZA). La Serena, Chile

⁴Departamento de Ciencias Geológicas, Universidad Católica del Norte. Antofagasta, Chile.

10 ⁵Departamento de Ciencias Históricas y Geográficas, Universidad de Tarapacá. Arica, Chile.

Correspondence to: Adriana Aránguiz-Acuña (aaranguiza@academicos.uta.cl)

Abstract. High Mountain Lakes in the Central Andean Altiplano experienced significant fluctuations in water levels during the Late Quaternary, which have affected the composition of aquatic communities. In this study, Casiri Hembra and Casiri Macho Lakes (Northern Chile, > 4,800 m a.s.l.) sediment cores were obtained and analyzed by combination of different
15 proxies: analyses of geochemistry, magnetic properties, and pollen assemblage, joint to ecological proxies, such as the structure of benthic macroinvertebrates, to identify environmental changes that occurred in the Altiplano region during the late Holocene, with particular emphasis on distinguishing local influences from broader regional processes and their impacts on aquatic community structure and surrounding vegetation of these isolated high-mountain lakes. Results showed a progressive change in depositional dynamics from the Late Holocene to the present, 900 years in Casiri Hembra Lake, and over 3,000
20 years in Casiri Macho Lake. Older sediments show a general dominance of fine-grained sediments, with episodes suggesting the influence of high-energy clastic inputs, likely reflecting episodic flooding or increased basin runoff. Recent deposits indicate the development of low-energy lacustrine conditions, increased productivity, and reduced terrigenous input. Volcanic activity of the surrounding complex was recorded. The aquatic community of Casiri Lakes shows a significant replacement of taxa, from Ostracoda and Diptera in older sediments to Anostraca Crustacea in the most recent sediments. In addition, the
25 presence of local microhabitats for the observed community is noted. High sedimentation rates in Casiri Lakes suggest complementary depositional sources to authigenic processes, such as sustained atmospheric deposition, which likely represents a significant contribution to the sediment budget.

1 Introduction

The Andean Altiplano (14-22°S)-Puna (22-27°S) is a north-south-extending plateau in the Central Andes of South America,
30 located above 3,700 m a.s.l., flanked by the Western and Eastern Andes Ranges (Tapia et al., 2012), and borders Peru, Bolivia, Argentina, and Chile. The Dry Puna is an ecoregion that stretches from approximately 17 to 27°S, characterized by drier and

lower-stature shrubs and grasslands spreading from northern Peru to northern Chile and Argentina, featuring a marked dry and cold season during the austral winter (May–August) (García-Lino et al., 2023).

35 The Altiplano-Puna has evolved through multiple phases of tectonic uplift and crustal shortening (Isacks, 1988; Allmendinger et al., 1997; Jordan et al., 2010), and its morphology has been modified afterward due to continuous drainage and erosional processes. In addition, the Central Volcanic Zone (CVZ) of the Andes, a band of active volcanic chains parallel to the continental margin from Southern Peru to Central Chile (14°S–27°S) (Stern, 2004), has formed what are now reflected as volcanic chains at elevations of 5,000–6,000 m (Allmendinger et al., 1997) and extensive ignimbritic surfaces (De Silva, 1991).
40 These long-term processes, which include the input of volcanic material deposited in the basin bottom and the interaction of hydrothermal fluids originating from nearby geothermal and volcanic sources (Valero-Garcés et al., 1999; Telford et al., 2004; Sáez et al., 2007; Tapia et al., 2019). Also, the persistent action of erosion, together with the natural reorganization of drainage networks, has shaped the morphology of numerous large-scale fluvial-lacustrine basins (Garziona et al., 2006), thereby modifying the chemistry of the surrounding lakes (Sáez et al., 2007).

An estimated 20% of the world's lake ecosystems are designated as remote, high-mountain lake systems (located at > 1,000 m
45 a.s.l.) (Loria et al., 2020). These lakes are often sustained by the low permeability of crystalline bedrock, which limits water infiltration and promotes surface water retention (Catalán et al., 2006). Due to their proximity to cryospheric sources, high-mountain lakes are particularly susceptible to the effects of rising global temperatures (Reato et al., 2021). Melting and thawing processes are significantly transforming these systems, which represent both prominent geomorphic features and critical freshwater reservoirs (Reato et al., 2021; Lone and Balakrishna, 2023). Given current global warming trends, it is crucial to
50 identify past forcing factors to understand lacustrine processes and their future spatiotemporal dynamics.

High Mountain Lakes in the Central Andean Altiplano experienced significant water level fluctuations during the Late Quaternary, altering their surface area-to-volume ratios (Placzek et al., 2009); therefore, this region provides a key archive for studying Quaternary climate variability. Altiplano lakes and sedimentary records reveal humid phases (e.g., the end of the last glacial period) and arid episodes during the mid-Holocene, linked to anomalies in the Intertropical Convergence Zone (ITCZ)
55 (Grosjean et al., 2001; Baker et al., 2001; Placzek et al., 2006), in addition to regional factors, such as El Niño–Southern Oscillation (ENSO) variability (Polissar et al., 2013). All of these factors contributed to changes in lake levels, which, in turn, affected the composition of the planktonic communities inhabiting the lakes (e.g., Tapia et al., 2003). Regardless, very little is known about the effects of long-term lake-level variability on the functional properties, such as lacustrine productivity (Bao et al., 2015).

60 Altiplano's fragmented and isolated waterscapes have provided patches of local suitable habitats for the reproduction and refuge of many aquatic invertebrate species and terrestrial insects with aquatic larval stages (Collado et al., 2011, 2014; Jacobsen and Dangles, 2017). Life-history strategies and morphological traits variations are likely influenced by local environmental conditions and selective pressures, suggesting specific adaptations to the microhabitats of the Altiplano (Acuña-Valenzuela et al., 2024). In extreme northern Chile, in the Caquena sub-basin, the Casiri Lakes basins reveal a Pleistocene-
65 Holocene volcanic and glacial dynamics. Phylogenetic studies have suggested that recent isolation events in aquatic systems



occurred within the basin (Collado et al., 2011, 2014), producing high endemism in different invertebrate groups, *Orestias* fishes, and vegetation groups. Nevertheless, the ecological drivers of community differentiation in the Caquena sub-basin remain unresolved.

In arid and high-altitude environments, lacustrine sedimentation is not solely controlled by catchment-derived inputs but may also include a significant contribution from direct atmospheric deposition. Under conditions of limited vegetation cover, reduced runoff, and abundant fine-grained surface sediments, aeolian transport can become an efficient mechanism for delivering clastic material to lake basins (Last and Smol, 2001; Muhs, 2013). As a result, sediment accumulation in such systems may reflect a combination of hydrological and atmospheric processes, with important implications for interpreting sedimentary records of past environmental and climatic changes (Prospero et al., 2002; Mahowald et al., 2010).

In this study, the Casiri Lakes (Arica y Parinacota Region, Northern Chile) sediment cores were obtained and analyzed by a combination of different proxies: geochemistry, magnetic properties, and pollen assemblage, joint to ecological proxies, such as the structure of benthic macroinvertebrates, to identify environmental changes that occurred in the Altiplano-Puna region during the late Holocene, with particular emphasis on distinguishing local influences from broader regional processes and their impacts on aquatic community structure and surrounding vegetation of these isolated high-mountain lakes.

2 Methodology

2.1 Study site

The Casiri Lakes basin is located 12 km west of the Caquena village (18°3'S, 69°12'W) in, Arica and Parinacota Region, near the international border with Bolivia (Fig. 1a, b). Casiri Macho Lake (4,845 m a.s.l., 18°3'S, 69°5' W) is located on the southern flank of Kunturiri volcano. It is hydrologically connected to two neighboring bodies of water: Casiri Hembra Lake (4,813 m a.s.l., 18°4' S, 69°6' W) to the west, and Sora Pata Lake (4,930 m a.s.l., 18°3.8' S, 69°4.1' W) to the northeast. These lakes are interconnected by a gently sloping drainage system that runs through a stream. Casiri Macho Lake lies within a paraglacial basin shaped by extensive Pleistocene glaciation, during which paleoglaciers extended below 4,450 m a.s.l., as evidenced by moraines and fluvio-glacial deposits in the region (Ammann et al., 2001). Post-glacial aridification has since transformed the basin into a topographically confined system bordered by steep volcanoclastic slopes (Grosjean et al., 2001; Sáez et al., 2007). The lake's modern hydrology is based on meltwater from the Kunturiri snow-capped mountains, channeled through Sorapata Lake, where Casiri Macho discharges into Casiri Hembra Lake. The Casiri Macho Lake covers an area of 39.4 ha (0.39 km²), with a length of 753.54 m and a depth of 41 m. Casiri Hembra Lake covers an area of 83.8 ha (0.84 km²), with a length of 1229.6 m and a depth of 29 m (Fig. 1c).

The oldest unit in the study area corresponds to the Pleistocene-aged Condoriri Volcanic Complex (Plcl), mainly composed of pyroxene-andesitic lava flows affected by moderate to intense glacial erosion. ⁴⁰Ar/³⁹Ar dating yielded an age of 650 ± 70 ka (García et al., 2004). This unit crops out mainly north of both lakes (Fig. 1c). To the southwest of Casiri Macho Lake and



southeast of Casiri Hembra Lake, the Larancagua Volcanic Complex (PIII) crops out, consisting of andesitic to dacitic domes and lava flows assigned to the Pleistocene based on stratigraphic relationships and the degree of glacial erosion (Clavero et al., 2012). Along the western margin of Casiri Hembra Lake, the Pomerape Volcano (Plpd) is represented by dacitic domes displaying flow banding and mafic enclaves. K-Ar and $^{40}\text{Ar}/^{39}\text{Ar}$ ages indicate volcanic activity during the Middle to Late Pleistocene (Wörner et al., 1988; Clavero et al., 2004). Extensive glacial deposits (PIHg), associated with lateral, frontal, and ground moraines, overlie these volcanic units and are attributed to the Last Glacial Maximum during the Late Pleistocene (14–12 ka BP) (Ammann et al., 2001). During the Late Pleistocene and Holocene, lacustrine deposits (PIHI) accumulated mainly around Casiri Hembra Lake. These sediments are rich in organic matter and interbedded with peat and pyroclastic layers, reflecting hydrological fluctuations and volcanic inputs. In addition, recent alluvial and colluvial deposits (PIHa and PIHb), associated with gravitational and fluvial processes, are recognized throughout the area. Finally, a thin crust of Holocene evaporitic saline deposits (Hs) crops out south of Casiri Hembra Lake (Clavero et al., 2012, 2018).

2.2 Samples collection

Sampling fieldwork was conducted in December 2021 and in May 2022, at the beginning and end of the wet season in the Andean Altiplano, respectively. In December, surface water physicochemical parameters such as pH, conductivity, temperature, and total dissolved solids (TDS) were measured using a portable multimeter (Hanna-HI98194); in addition, filtered water samples were collected from the surface of lakes Casiri Hembra and Casiri Macho, primarily in littoral areas, with the aim of quantifying the main cations and anions. Five samples (CAH-1 to CAH-5) were obtained from Casiri Hembra, distributed across the northeastern, eastern, southern, and western sectors of the lake, including areas near the Kunturiri Volcanic Complex, lacustrine deposits, and an adjacent dacitic dome. Surface water sample CAH-5 was collected at the extraction point for sediment core CAH-SHC-2. Two surface samples (CAM-1 and CAM-2) were collected from Casiri Macho in the lake surface discharge zone, both from the same sampling point. Water samples were filtered in the field using 0.22 μm syringe filters and Luer-Lok syringes, then kept at 4°C until analysis. In the May fieldwork, Casiri Hembra Lake and Casiri Macho Lake were coring sampled. The specific coring sampling point for each lake was selected based on bathymetry previously generated using a Garmin EchoMap Plus 42CV (Fig. 1c).

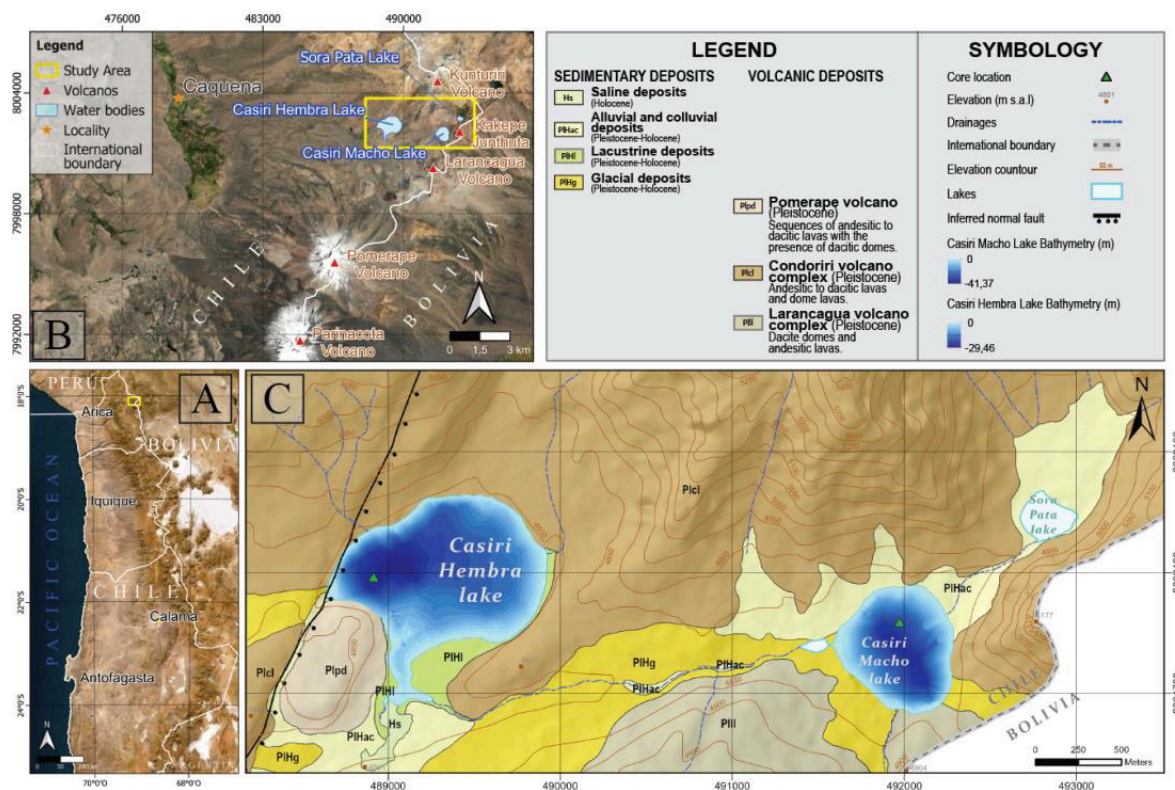


Figure 1: Location of the Caquena sub-basin in the Arica y Parinacota Region, Northern Chile (a). Location of the selected lakes for this study (b). Geological map of the Caquena sub-basin, showing Casiri Macho, Casiri Hembra, and Sorapata Lakes, based on Clavero et al. (2012), including bathymetries of Casiri Macho and Casiri Hembra Lakes (c).

125 One sediment core was obtained from the deepest part of each lake, where the highest sedimentation rates are expected. In Casiri Hembra Lake, the deepest point was at 29 m, and the obtained core, CAH-SHC-2, measured 95 cm in length. Meanwhile, in Casiri Macho Lake, the deepest area was located at 41 m, and the core CAM-SHC-2 measured 128 cm in length. The cores were obtained using a UWITEC gravity corer (9 cm in diameter), operated from a surface platform. The cores were transported in a PVC casing to prevent vertical movement and control temperature until they arrived at the Center of Advanced Research in Arid Zones (CEAZA) in La Serena, Chile. The cores were stored at 4°C, underwent longitudinal splitting, photographing, and X-ray imaging (Appendix Fig. A1).

130

2.3 Age-depth models

The chronology was established through radiocarbon (¹⁴C) dating using Accelerator Mass Spectrometry (AMS) on bulk sediment at the Direct AMS laboratory in the USA. The dates were calibrated against the Southern Hemisphere curve (SHCal20; Hogg et al., 2020), and the age-depth model was constructed using the Bacon package (Blaauw and Christen, 2011) with default settings.

135



2.4 Water physicochemical properties and sediment analysis

Main cations and anions of lake waters were measured by liquid chromatography using a METROM ECO IC Package. HCO₃⁻ and CO₃²⁻ were analyzed by acidimetric titration with HCl 0.1 M. Ionic balance error was lower than 10%.

140 Grain size was measured at 1 cm intervals from sediment samples using laser diffraction to determine particle distribution with a MasterSIZER 2000 at the Department of Geology, Universidad de Chile. Data processing was performed with Hydro2000 software, and grain size classification followed the Udden-Wentworth scale (Tucker, 2009).

Elemental depth distribution was qualitatively estimated using an XRF Core Scanner (Avaatech XRF Core Scanner, sixth generation) at Universidad de Concepción. Each core section was covered with a 4 μm thick Ultralene® plastic film to prevent
145 contamination and protect the detector window. Measurements were taken at 0.5 cm resolution, covering 90 cm of CAH-SHC-2 and 112 cm of CAM-SHC-2. The instrument settings are as follows: Voltage (kV): 10; 20; 50; Count time (s): 27; 40; 39; Filter: no filter; Pd-thin; Cu. Raw data, expressed as element intensities in counts per second (cps) per centimeter, were subsequently corrected using the centered log-ratio (clr) transformation to minimize bias from matrix effects and the closed-sum constraint (e.g., Weltje et al., 2015; Lee et al., 2019; Schwestermann et al., 2020; Bertrand et al., 2024).

150 Organic, inorganic, and carbonate matter content were estimated by the loss on ignition (LOI) test (Heiri et al., 2001) at 1 cm contiguous intervals. Sediment samples were placed in pre-weighed crucibles and oven-dried to constant weight for 24h at ca. 105°C, after which they were removed and allowed to cool to room temperature in a vacuum desiccator. Once cooled, they were reweighed primarily to ensure the samples were fully dried before determining their organic and carbonate contents. The process was repeated at 550°C and 950°C, and the percentages of organic matter and carbonates was calculated using Eqs. 1
155 and 2, respectively.

$$\text{LOI}_{550} = ((\text{DW}_{105} - \text{DW}_{550}) / \text{DW}_{105}) * 100 \quad (1)$$

Where LOI₅₅₀ represents LOI at 550 °C (as a percentage), DW₁₀₅ represents the dry weight of the sample before combustion, and DW₅₅₀ the dry weight of the sample after heating to 550 °C (both in g). In a second step, carbon dioxide is evolved from carbonate, leaving oxide, and LOI is calculated as:

160
$$\text{LOI}_{950} = ((\text{DW}_{550} - \text{DW}_{950}) / \text{DW}_{105}) * 100 \quad (2)$$

Where LOI₉₅₀ is the LOI at 950 °C (as a percentage), DW₅₅₀ is the dry weight of the sample after combustion of organic matter at 550 °C, DW₉₅₀ represents the dry weight of the sample after heating to 950 °C, and DW₁₀₅ is again the initial dry weight of the sample before the organic carbon combustion (all in g). The weight loss by LOI at 950 °C, multiplied by 1.36, should theoretically equal the weight of the carbonate in the original sample (Bengtsson and Enell, 1986).

165 The magnetic susceptibility (k) of sediments was analyzed at 1 cm intervals using a Kappabridge MFK1_FA instrument (AGICO Co) in the Paleomagnetism Laboratory of the Geology Department, Universidad de Chile. This was measured under environmental conditions (22–24 °C) and a magnetic field of 200 A/m. The samples were measured at two different frequencies: 976 Hz (low frequency; klf) and 15,616 Hz (high frequency; khf). In this study, the parameter k is equivalent to



klf. The magnetic susceptibility dependent on the frequency (kfd%) was calculated using both χ_{lf} and χ_{hf} ($kfd\% = (klf - khf /$
170 $klf) \times 100\%$; Dearing et al., 1996).

The magnetic mineralogy was determined through thermomagnetic experiments (magnetic susceptibility as a function of
temperature). Two representative sediment samples from Casiri Hembra (18 and 66 cm depth) and Casiri Macho (9 and 86 cm
depth) Lake were selected for analysis at the Magnetism Laboratory of Geoscience Environmental Toulouse (GET). The
experiments were conducted using a CS3 furnace coupled to a KLY5 susceptometer (AGICO Co.), applying a weak magnetic
175 field (300 A/m), at 1 atm pressure and under a helium atmosphere. Each sample was heated from room temperature (~ 25 °C)
to approximately 700 °C and subsequently cooled back to room temperature. Curie temperatures were determined following
the method of Hodel et al. (2017), based on the calculation of the gradient $|(KT_{n+1} - KT_n) / (T_{n+1} - T_n)|$.

2.5 Biological proxies

Pollen records were analyzed at 4 cm intervals in both cores CAH-SHC-2 and CAM-SHC-2. A 1 cm³ volume of sediment
180 from each sample was processed according to standard laboratory techniques, including KOH, HF, and acetolysis treatments
(Faegri and Iversen, 1989). Tablets of the exotic spore *Lycopodium clavatum* were added to each sample to calculate pollen
concentration (grains·cm⁻³) (Stockmarr, 1971) and pollen influx (grains·cm⁻³·yr⁻¹). Pollen grains were identified at 400x and
1000x magnification using the pollen reference collection of the Laboratory of Palynology at CEAZA and reference pollen
books (Heusser 1971; Markgraf and D'Antoni 1978; Villagrán 1980). The basic pollen sum for each level includes at least 300
185 terrestrial pollen grains (trees, shrubs, grasses, and herbs) per sample, excluding aquatic and paludal pollen types and fern
spores.

Benthic invertebrates were separated, identified, and counted from each centimeter of sediment cores, totaling 93 samples
from CAH-SHC-2 and 125 from CAM-SHC-2. A 210 µm sieve was used to clean the samples. The samples were preserved
in 70% alcohol and observed under a stereomicroscope with a maximum magnification of 90x. The GBIF database was used
190 for taxonomic classification.

2.6 Statistical analysis

To analyze associations between sediment chemical variables, a Stratigraphically Constrained Cluster Analysis (CONISS) and
Principal Component Analysis (PCA) were applied to the clr-transformed XRF dataset. Previously, a Spearman correlation
was performed; strongly correlated variables (> 0.7) and, therefore, collinearity between them were considered when filtering
195 the explanatory variables (Appendix Fig. A4). Thus, sedimentary variables (grain size, magnetic susceptibility, and Organic
Matter [OM]) were not included as active variables in the clustering and ordination analyses. The sedimentary variables were
subsequently projected onto the ordination space of the PCA figure using the *envfit* function in the *vegan* package (Oksanen



et al., 2026). PCA was performed using Euclidean distance to visualize the distribution of variance among clusters obtained by CONISS analysis, implemented with the vegan and rioja packages (Juggins, 2024).

200 To evaluate the benthic invertebrate community, the identified taxonomic groups were classified according to functional similarities and Hellinger-transformed (Legendre and Legendre, 2012) using the vegan package. Community turnover was assessed using the rate-of-change method implemented in the RRatepol package (Mottl et al., 2021), applying a moving-window approach with 100-year time bins and the Chord dissimilarity coefficient. All statistical analyses were conducted in R (version 4.5) (R core Team, 2025).

205 3 Results

3.1 Age-depth models

A total of four radiocarbon (^{14}C) dates spanning 888 cal yr BP were obtained from CAH-SHC-2, and six dates spanning the past 3,052 cal yr BP were obtained from CAM-SCH2. The resulting age-depth models indicate a relatively linear relationship of both records (Appendix Fig. A1), suggesting a consistent deposition rate throughout the entire records, estimated as 0.1
210 $\text{cm}\cdot\text{yr}^{-1}$ for CAH-SHC-2 and $0.05 \text{ cm}\cdot\text{yr}^{-1}$ for CAM-SCH-2, as illustrated in the central panels of Appendix Fig. A1.

3.2 Water physicochemical properties and sediment analysis

The results of standard physico-chemical parameters of surface water in Casiri Hembra and Casiri Macho Lake are presented in Table 1. In general, the water of Casiri Macho was colder, less conductive, and contained a lower proportion of TDS than in Casiri Hembra. Both lakes presented alkaline pH (Table 1).

215

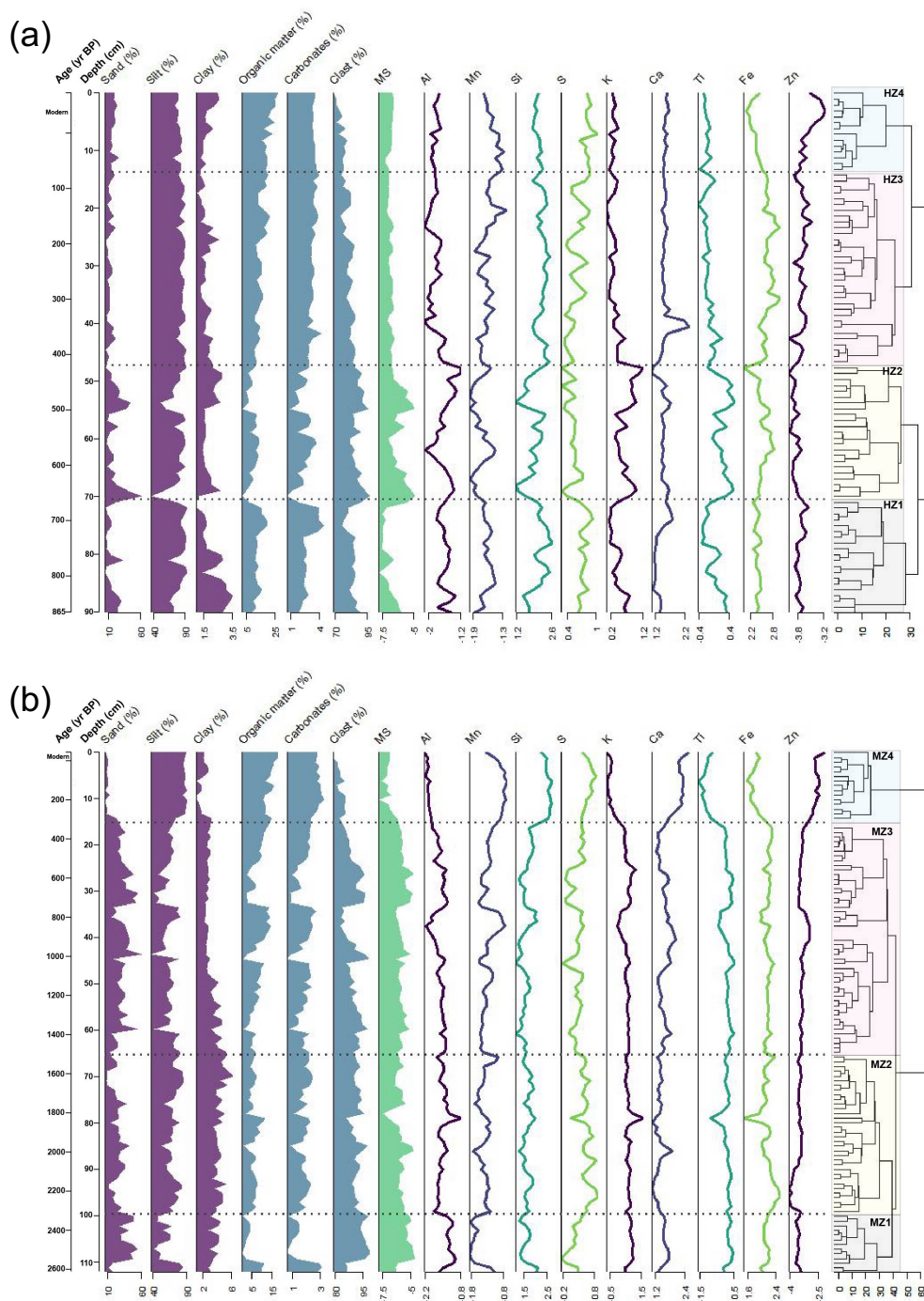
Table 1. Physical and chemical parameters of surface water of Casiri Macho and Casiri Hembra Lakes.

Parameter	Casiri Hembra (CAH)					Casiri Macho (CAM)				
	Mean	Median	Min	Max	SD	Mean	Median	Min	Max	SD
Ca^{2+} (mg/L)	100.176	102.06	91.08	108.02	6.30	34.86	34.86	32.32	37.4	3.59
Mg^{2+} (mg/L)	35.152	35.68	30.7	38.44	3.26	8.055	8.055	7.55	8.56	0.71
K^{+} (mg/L)	7.674	7.588	7.042	8.382	0.63	2.159	2.159	1.8	2.518	0.51
Na^{+} (mg/L)	43.358	43.43	37.91	47.7	3.89	5.21	5.21	4.34	6.08	1.23
SO_4^{2-} (mg/L)	307.686	310	293.51	315.4	8.94	-	-	-	-	-
Cl^{-} (mg/L)	61.632	61.54	59.23	63.85	2.00	-	-	-	-	-
HCO_3^{2-} (mg/L)	107.4	106.1	100	116	6.01	-	-	-	-	-
T ($^{\circ}\text{C}$)	15.562	14.160	10.100	23.010	5.16	7.41	7.41	7.41	7.41	0
CE (mS/cm)	1.142	1.146	1.096	1.174	0.03	0.682	0.682	0.682	0.682	0
TDS (mg/L)	571	573	548	587	14.29	339	339	339	339	0
pH	9.254	9.21	8.94	9.62	0.25	9.42	9.42	9.42	9.42	0



220 Sediment analysis results are summarized in Figure 2 and Appendix Fig. A2. LOI results showed that the sediment content in both lakes is predominantly clastic (83% in Casiri Hembra and 90% in Casiri Macho), followed by organic matter (14% in Casiri Hembra and 8% in Casiri Macho), and carbonates < at 3% in both lakes. In both cores, a slight increase in the percentage of organic matter was observed from the bottom to the top, but in no case did it exceed 25%.

225 The grain-size analysis of Casiri Hembra Lake showed a mean size of 32.5 μm , classifying the sediment as silt. Grain sizes range from 22.6 μm to 103.6 μm , encompassing the clay-to-sand fractions, with no gravel detected. The distribution of sediment fractions showed a higher proportion of silt throughout the core, with clearly differentiated sand peaks below 50 cm. At Casiri Macho Lake, the mean particle size was 32 μm (silt), with overall grain sizes ranging from 13.5 μm to 75 μm , spanning the clay-to-sand fractions. The distribution of sediment fractions showed a higher proportion of silt throughout the core, particularly in the uppermost part, with an average grain size of 25 μm . A higher proportion of the sand fraction is observed, with peaks reaching 50%, at depths greater than those covered by the Casiri Hembra core (Fig. 2).



230 **Figure 2: Geochemical profiles (lines) with CONISS clusterization and sedimentary variables (shaded profiles) plot obtained from Casiri Hembra Lake (a) and Casiri Macho Lake (b).**



Both sediment core records, CAH-SHC-2 from Casiri Hembra (Fig. 2a) and CAM-SHC-2 from Casiri Macho (Fig. 2b) (Appendix Fig. A2) showed four CONISS-separated stratigraphic zones with distinctive textural and geochemical characteristics. For greater clarity in identifying the zones of each sediment core, CAH-SHC-2 zones were designated HZ1-
235 HZ4, while the zones defined for CAM-SHC-2 are designated MZ1-MZ4 from the deepest to most surface.

In CAH-SHC-2, Zone 1 (HZ1) (71-93 cm; 660-897 cal yr BP) is characterized by high silt (~78%), a low clay content (~2.4% on average) but slightly higher than the overlying intervals, and intermediate organic matter and carbonate content (LOI550 = 12%, LOI950 = 2.6%). XRF signals showed slightly high Si content. The overall geochemical background is stable, mainly in Al, Fe, Zn, with small-amplitude peaks, where it also occurs with the content of sand and MS, which could indicate the input
240 of iron and silicate-rich detritus under relatively low to moderate depositional energy. Although HZ1 corresponds to a layer of discrete organic and carbonate content, suggesting low productivity, an increase in organic matter and carbonates is observed at the upper limit of the horizon. Overall, HZ1 records predominantly fine-grained, terrigenous depositional regimes with short-duration disturbances (small clastic pulses).

HZ2 (48-71 cm; 423-660 cal yr BP) is characterized by containing the most pronounced coarse-grained, high-energy evidence
245 of the sedimentary core. HZ2 exhibits two clear events of high sand content (>30-60%), marked increases in magnetic susceptibility, and decreases in organic matter and carbonate content, at the bottom (~70 cm depth) and the top (~49 cm depth) of the horizon. These sand-rich horizons show the highest levels of K and Ti in the entire record, in concordance with the minimum of Mn, Si, and S. The combination of a high sand fraction and magnetic susceptibility is consistent with a rapid input of coarse and dense minerals (feldspar and tephra/lithic fragments), related to possible episodic flooding, debris flow, volcanic
250 eruptions or mass transport events into the lake.

HZ3 (15-48 cm; 82-423 cal yr BP): This zone is characterized by markedly thinner grain size and growing organic matter content, compared to HZ2. In HZ3, sand and clasts decrease substantially, while OM and carbonates are more variable, increasing towards the top of the horizon. The low magnetic susceptibility and coarser material observed suggest a period of reduced clastic delivery and/or erosion in the catchment. Element profiles in HZ3 show relatively high concentrations of Si
255 and Fe, and the highest concentrations of Mn. A reduction in Al, K, and Ti is also observed, along with a slight and sustained increase in Zn and S. These variations suggest a transition to a low-energy regime, with preservation of organic matter and carbonate. At ~40 cm depth, a large Ca peak is highlighted.

HZ4 (0-15 cm; modern-82 cal yr BP): The upper zone is the thinnest and richest in organic matter in the sedimentary core. Clay increases and magnetic susceptibility remains low, as in HZ3. Elemental patterns show Si, Ca, and Ti content similar to
260 that of HZ3, but with a rapid decrease in Fe and Mn content. There is a notable increase in S and a higher Zn peak during the last period. These characteristics indicate low-energy depositional conditions dominated by autochthonous sedimentation and organic accumulation in the modern lake environment.

In CAM-SHC-2, Zone 1 (MZ1) (103-128 cm; 2,395–3,052 cal yr BP) shows a marked internal transition in sediment characteristics. The deeper portion of the zone is dominated by fine-grained sediments composed primarily of silt, organic
265 matter, and carbonate contents. Overall, in this zone, geochemical profiles are marked by short-term peaks and troughs. At



~105 cm depth a pronounced change occurs, grain size shifts from silt to sand, while both organic matter and carbonate decline, and clastic fragments and magnetic susceptibility increase. This pronounced change coincides with an increase in Al, K, Ca, Ti, and Fe, while Mn, Si, and S decrease.

270 In MZ2 (69-103 cm; 1,708–2,395 cal yr BP) is dominated by fine to moderately fine sediments, with silt remaining the principal grain-size fraction. A clear event occurs at ~79 cm, where sand and organic matter decrease, and clasts increase. Here, Al and K show an abrupt peak, while S, Fe, and Ti show a marked drop, possibly corresponding to a thin layer of volcanic ash/tephra or feldspar-rich debris.

275 MZ3 (18–69 cm; 404–1708 cal yr BP) represents the thickest portion of the CAM-SHC-2 sequence and exhibits great variability in sedimentological proxies. Grain-size distributions show silt peaks, alternating with layers of increased sand fractions, occasionally accompanied by visible clasts. These coarser layers are associated with peaks in magnetic susceptibility, indicating episodic input of denser detrital material (~31, ~43, ~60 cm depth). Elemental variations also reflect these pulses with localized increases in Al, Ti, and K, and a drop in Mn, Si, and S in the sandier horizons.

280 MZ4 (0–18 cm; modern–404 cal yr BP) represents the most recent depositional conditions and is characterized by the highest proportion of fine-grained sediments, carbonates, and organic content in the core. Sand and clay fractions, together with magnetic susceptibility, remain very low, whereas silt predominates. Al, K, Ti, and Fe decrease to their lowest levels here, while Mn, Si, S, Ca, and Zn reach the highest relative abundance through the core.

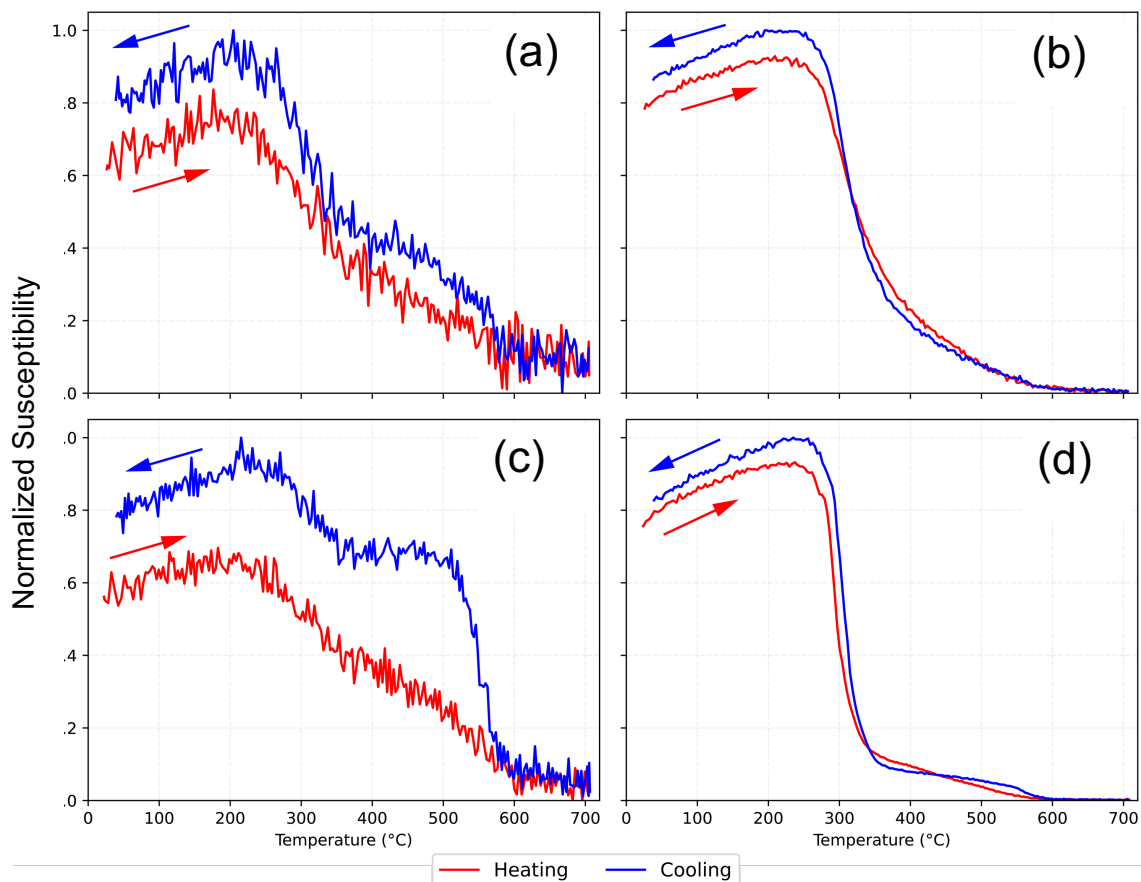
In summary, the CAM-SHC-2 is a longer and more compressed record than the CAH-SHC-2; nevertheless, variations observed in the CAH-SHC-2 agree with those observed in the first 45 cm of the CAM-SHC-2. In both, a stratigraphic succession records progressive change in depositional dynamics from the Late Holocene to the present. At the base, CAM-SHC-2 is dominated by fine-grained sediments but is interrupted by episodes of coarser material and fluctuations in key geochemical proxies (at 285 107, 100, 87, 60, 42, and 33 cm, corresponding to 2500, 2350, 2000, 1400, 1000, and 70 yr BP, respectively). These intervals suggest the influence of high-energy clastic inputs, likely reflecting episodic flooding or increased basin runoff. Toward the surface, the record is dominated by silt-rich sediments with higher concentrations of organic matter and carbonates, even though the sum of both never exceeds 25%. These deposits reflect the development of low-energy lacustrine conditions, with increased lacustrine productivity or higher pH (as observed in the current water column), and reduced terrigenous input.

The magnetic susceptibility profiles remain negative in both lake cores, indicating that they correspond to diamagnetic materials. The observed magnetic susceptibility peaks align with the sand peaks and clasts, in the granulometric and LOI profiles, respectively, suggesting a detrital origin and potentially indicating greater sediment input from outside the basin or lower authigenic mineral formation intensity (Fig. 2; Appendix Fig. A2).

295 Thermomagnetic curves from Casiri Hembra (18 and 66 cm; Figure 3a and 3b, respectively) and Casiri Macho (9 and 86 cm; Figure 3c and 3d, respectively) show overall similar shapes. The shallow samples from both lakes are characterized by low magnetic susceptibility values and relatively high noise levels, indicative of low concentrations of ferromagnetic minerals, whereas the deeper samples show higher magnetic mineral concentrations, consistent with bulk magnetic susceptibility values (Fig. 2). In both lakes, susceptibility progressively decreases from approximately ~280–300 °C to ~580–600 °C, followed by



300 a sharp decline toward near-zero values at higher temperatures. The samples from Casiri Hembra and the deeper sample from
Casiri Macho (86 cm; Fig. 3d) exhibit largely reversible thermomagnetic behavior, with the heating and cooling curves
overlapping closely. In contrast, the shallow Casiri Macho sample (9 cm; Fig. 3c) exhibits a clearly irreversible response. The
deeper samples (Fig. 3b and Fig. 3d) show a well-defined susceptibility drop near $\sim 300^\circ\text{C}$, whereas reliable Curie temperatures
could not be confidently determined for the shallow samples due to their low signal-to-noise ratio. The predominantly
305 reversible behavior observed in three of the four samples suggests that heating did not induce significant mineralogical
transformations, consistent with the presence of thermally stable magnetic phases. On the other hand, the irreversible behavior
observed in the shallower Casiri Macho sample is interpreted as resulting from mineralogical changes during heating,
potentially involving the neoformation of magnetic minerals from precursor iron-bearing phases. This process may be favored
by the higher abundance of iron hydroxides and organic matter in near-surface sediments, which are more susceptible to
310 thermal alteration. Although the experiments were conducted under a helium atmosphere, oxygen adsorbed onto grain surfaces
or trapped within pore spaces may promote partial oxidation during heating. The susceptibility decay observed between ~ 280
and $\sim 350^\circ\text{C}$, particularly in the deeper samples from both lakes, is compatible with the thermal destabilization of greigite. The
more gradual decay extending toward $\sim 580\text{--}600^\circ\text{C}$ suggests a subordinate contribution from magnetite or low-Ti
titanomagnetite, and may also indicate the presence of a slightly more oxidized magnetic phase. In the deeper Casiri Hembra
315 sample there is a less pronounced susceptibility decrease between ~ 350 and $\sim 580^\circ\text{C}$ compared to the deeper Casiri Macho
sample, which may reflect a higher proportion of titanomagnetite. As this phase is unlikely to form under reducing authigenic
conditions, it probably has a detrital origin, suggesting greater external sediment input or lower authigenic mineral formation
than in Casiri Macho. Overall, considering both lakes, the surface samples show lower concentrations of ferromagnetic
minerals. The four samples, based on the shape of the thermomagnetic curves and supported by the magnetic susceptibility
320 values, suggest the presence of greigite; however, the deeper samples show a higher proportion of this mineral, which may
indicate an authigenic origin. Furthermore, the Casiri Macho samples appear to be characterized by a greater abundance of
greigite compared to those from Casiri Hembra.



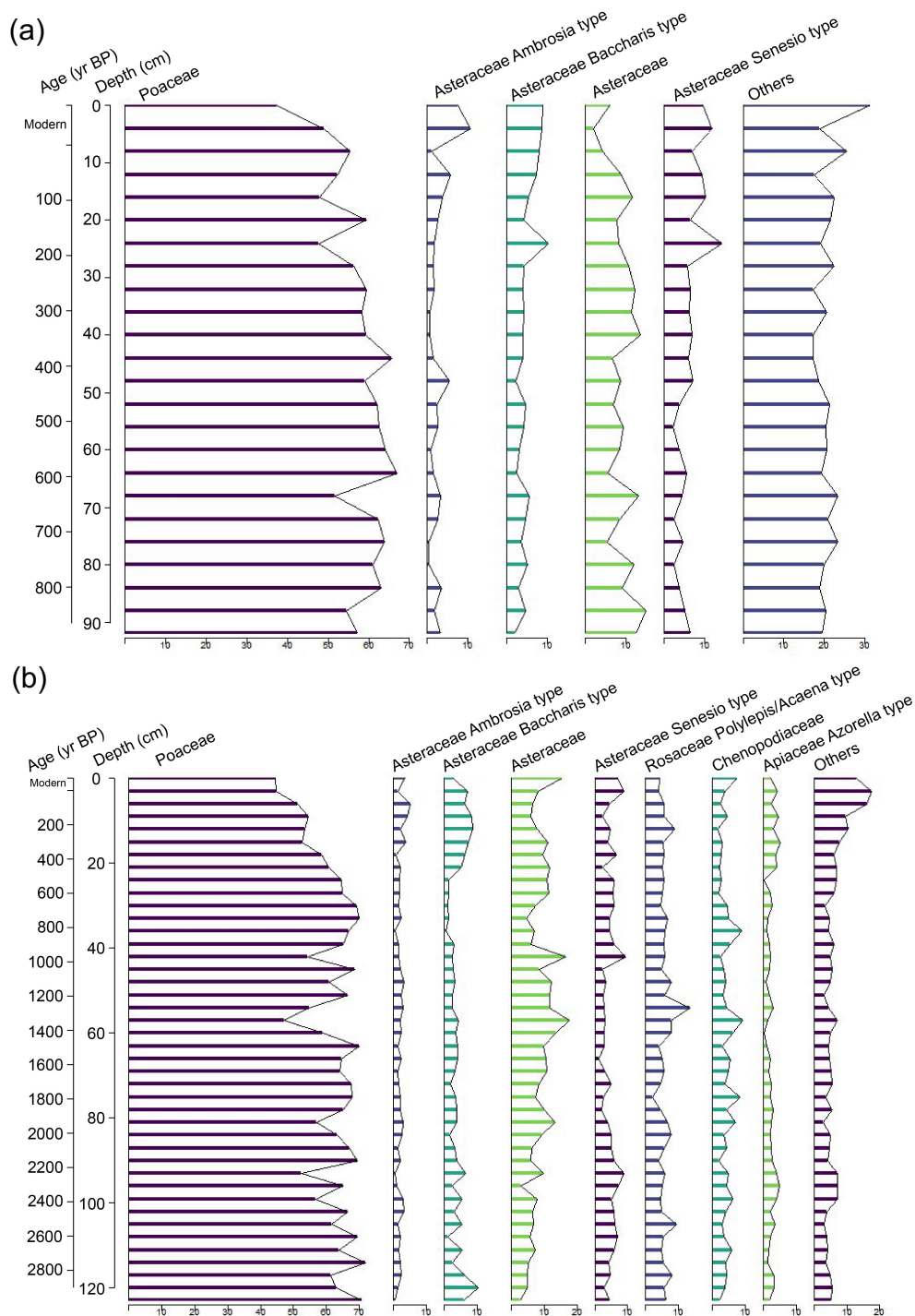
325 **Figure 3: Curves obtained from thermomagnetic experiments (magnetic susceptibility as a function of temperature) from Casiri Hembra: 18 and 66 cm depth; (a) and (b), respectively; and Casiri Macho: 9 and 86 cm; (c) and (d), respectively**

3.3 Biological proxies

The pollen record in both lakes was done, Casiri Hembra (Fig. 4a) with age of 900 yr BP, and Casiri Macho Lake (Fig. 4b) with an age of 3,000 yr BP. Both lakes show the same general trend, with dominance of Poaceae, different Asteraceae types and Rosaceae *Polylepis/Acaena* type. Thus, the Casiri Macho record shows, between approximately 3,000 and 2,200 yr BP, a dominance of Poaceae, though with a relatively higher presence of Asteraceae *Baccharis*-type, Asteraceae near the base of the record and subsequently relatively high values of Asteraceae *Senecio*-type (Fig. 4b). Both indicators could suggest a relatively higher presence of taxa associated with the Puna zone, in relation to the High Andean Steppe. High percentages of Poaceae between approximately 2,100 and 800 yr BP could suggest a greater presence of the High Andean Steppe zone, though this indicator declined around 1,500 yr BP when increasing *Polylepis/Acaena* pollen. Subsequently, the decline in Poaceae pollen and the increase in *Baccharis*-type Asteraceae, Apiaceae, and ragweed-type Asteraceae could suggest the expansion of the lower vegetation belt. Particularly, around 550 yr BP the increase of Asteraceae *Baccharis* type and Apiaceae *Azorella* type reinforce this trend.

330

335



340 **Figure 4: Profiles of main pollen types, relative abundances in zonation based on CONISS cluster analysis for (a) Casiri Hembra and (b) Casiri Macho Lake.**



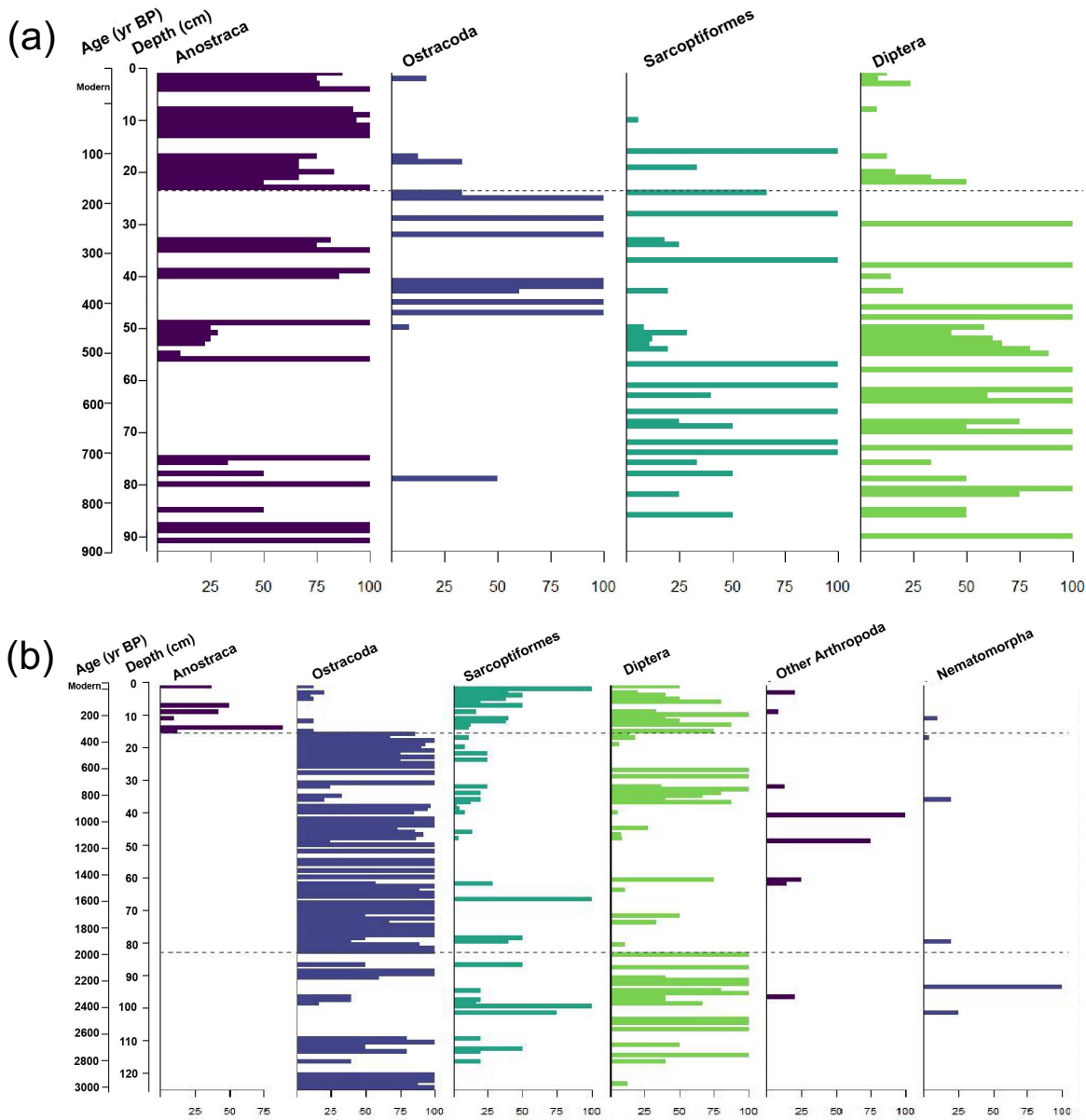
The distribution of invertebrates throughout the entire CAH-SHC-2 core is characterized by the relative abundance of fossil records of Anostraca (52.8%), Diptera (28%), Sarcoptiformes (11.9%), and Ostracoda (7.2%). The relative abundance throughout the entire CAM-SHC-2 core shows the following distribution: Ostracoda (65.6%), Diptera (19.9%), Sarcoptiformes (9.4%), Anostraca (2.7%), f. Nematomorpha (1%), Coleoptera (0.3%), Plecoptera (0.1%), and other Arthropoda (1%).

345 Although the proportions of dominant taxa varied between Anostraca and Ostracoda, the frequency of Sarcoptiformes and Insecta (grouping Diptera, Coleoptera, and Plecoptera) was similar in both lakes. A greater invertebrate diversity and taxonomic richness were recorded in sediment cores from Casiri Macho (mean Shannon index = 0.2788; mean richness = 1.468) relative to Casiri Hembra (mean Shannon index = 0.2159; mean richness = 1.204).

Figure 5 shows the profiles of macroinvertebrate relative abundances by depth for each core. In Figure 5a, Anostraca are present throughout the Casiri Hembra sediment record, with greater abundance in the recent period, since 200 yr to the present.

350 The other three relevant groups reach higher and more regular abundances between 900 and 200 yr BP and are scarcer in the recent deposit. In Figure 5b, it is observed that Ostracoda were more variable in the deepest sediments (between 3,000 and 2,000 yr BP), very abundant between 2,000 and ~400 yr BP, and rare since ~400 yr BP to the present. The opposite pattern is observed in Anostraca, which was exclusively found in the current period (~400 yr BP to nowadays). The other two dominant

355 groups, the mites of the Sarcoptiformes and the insects of the order Diptera, showed variation across the record, with greater abundances and regularity between 3,000 and 2,000 yr BP, and during the recent period (~400 yr BP to nowadays). This turnover between taxa is reflected in significant values of the RoC statistic. In the Casiri Hembra record, there was one significant value, at 1,037 yr BP $RoC_{CAH} = 1.414$ [0.221-1.414]. Meanwhile, in the Casiri Macho Lake record, there were two significant RoC values, at 296 yr BP $RoC_{CAM} = 1.303$ [1.407-0.065], and at 936 yr BP $RoC_{CAM} = 1.014$ [1.408-0.087].



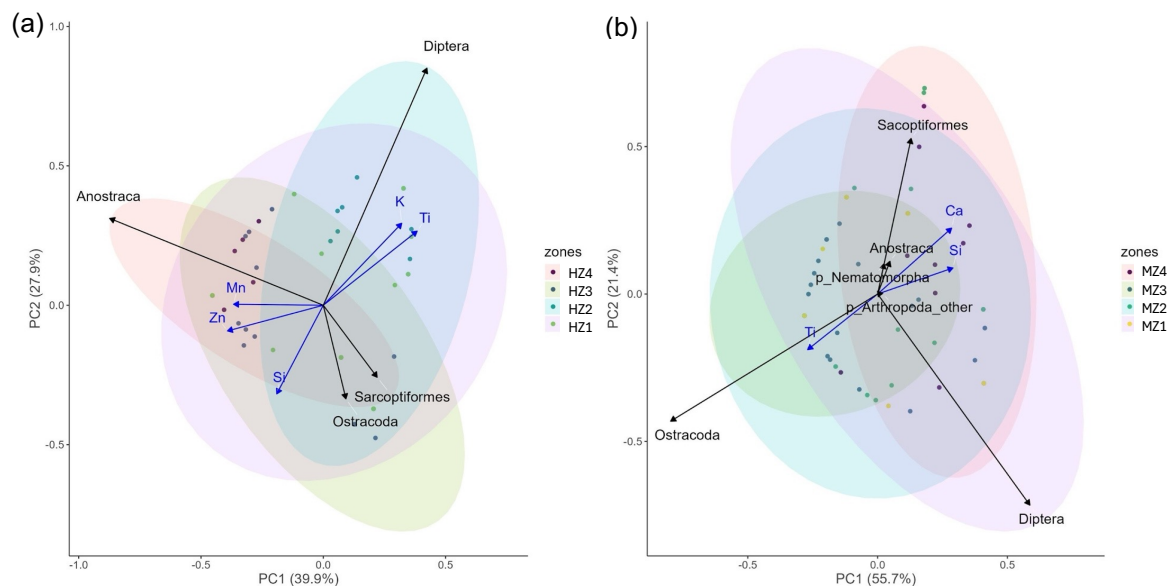
360

Figure 5: Temporal profiles of main benthic invertebrates, relative abundances in zonation based on CONISS cluster analysis for (a) Casiri Hembra and (b) Casiri Macho Lake.

In the PCA of invertebrates results and inorganic indicators (Fig. 6), the main groups recorded in CAH-SHC-2, Anostraca and Ostracoda, are displayed in opposite directions (Fig. 6a). The Anostraca group is more strongly associated with Zn and Mn (Fig. 6a). Sarcoptiformes and Ostracoda are closely associated variables and weakly associated with Si. Diptera, in the first quadrant, is associated with K and Ti. In the PCA of CAM-SHC-2 (Fig. 6b), the selected variables explain more than 77% of the variance in the data. The three main taxa are distributed in different quadrants. Ostracoda are thoroughly associated with



Ti, while Sarcoptiformes, Anostraca, and the other less-represented groups are associated with Ca and Si. The abundance of Diptera, in change, is not associated with any significant geochemical variable.



370

Figure 6: Principal Component Analysis of macroinvertebrates abundances and geochemical variables, and clumped by CONISS zones, for cores from (a) Casiri Hembra and (b) Casiri Macho Lake.

4 Discussion

This study provided the first-ever sedimentary records from two lakes at the northernmost tip of the Chilean Altiplano, at high altitudes >4,800 m a.s.l.: Casiri Hembra and Casiri Macho Lakes, located on the border with Bolivia. Our results showed similarities between cores from both lakes: variations observed in the shorter core from Casiri Hembra agree with those in the first 45 cm of the Casiri Macho core. In both, a progressive change in depositional dynamics from the Late Holocene to the present is observed, 900 years in Casiri Hembra Lake, and over 3,000 years in Casiri Macho Lake. Older sediments show a general dominance of fine-grained sediments, with episodes suggesting the influence of high-energy clastic inputs, likely reflecting episodic flooding or increased basin runoff. Recent deposits indicate the development of low-energy lacustrine conditions, increased productivity, and/or reduced terrigenous input.

Specifically, in Casiri Macho core (at ~79 cm depth, ~1800 yr BP), there is a clear event in which Al and K show an abrupt peak, while S, Fe, and Ti show a marked drop, possibly corresponding to a thin layer of volcanic ash/tephra or feldspar-rich debris. This localized layer could indicate the input of minerals such as feldspars, Fe-Ti oxides, and calcite, which suggest volcanic ash falls (Sabatier et al., 2022). The continuous fine-grained sediments and stable elements suggest a depositional environment dominated by background sedimentation under relatively stable hydrological conditions. Overall, this interval reflects relatively consistent lacustrine sedimentation with limited but episodic detrital input. Engel et al. (2014) identified a

385



period of stable temperatures between 2,750 and 1,950 yr BP from a *Distichia* peat core obtained from Western Cordillera of the Central Andes, Southern Perú, than coincides with inferred drier conditions associated with increased dust levels in the Sajama ice core (Thompson et al., 1998), and warm and wetter episodes around 1,880, 1,320 and 1,010 yr BP. Pollen record of Chungara Lake, also suggests humid conditions from 2,200 until 1,500 yr BP (Jara et al., 2019), while other proxies, such as rodent middens from Cuesta Chita, show similar trends with end of humid period around 1,000-700 yr BP (Jara et al., 2020; de Porras et al., 2021).

Later, between 600 and 400 yr BP, there is an increase in Ti, Al, and K and a decrease in Ca, S, and Zn. Also, during this period, an increased clast fraction in the sediments, coarser grains (clay and sand), and peaks in magnetic susceptibility were observed. All these variations could be associated with an increased snowmelt associated with warmer periods, resulting in catchment runoff, greater detrital contribution and sediment input from outside the basin. Increased humidity and catchment runoff in the Altiplano and Atacama region commonly enhance erosion and terrigenous sediment transport into lacustrine systems, producing higher detrital input, coarser grain sizes, and increased magnetic susceptibility (e.g., Grosjean et al., 1995; Nester et al., 2007). This period is also marked by the onset of the decline in Poaceae pollen and by increases in *Baccharis*-type Asteraceae, Apiaceae, and *Ambrosia*-type Asteraceae, as indicators of less humidity, such as in lower vegetational floor. The predominance of Poaceae, with Asteraceae as a secondary component, reflects modern Puna-type vegetation, characteristic of current high-elevation grassland ecosystems that dominate the Puna region and adjacent areas (Jara et al., 2020).

Following that period, for the most recent horizons up to the present day, both lake records show a strong decrease in Al, K, Ti, and Fe, a replacement from coarse- to fine-grained material, and from clasts to organic matter. In addition, increases in Mn, Si, S, Ca, and Zn suggest calcite precipitation or evaporative conditions, indicating drier modern conditions. Modern Casiri Macho sediments reflect a predominance of organic-rich fine-grained sedimentation, consistent with a transition to more productive lacustrine conditions and a decrease in detrital input. The reduced magnetic susceptibility allows us to infer a limited input of basin-derived ferromagnetic minerals. Overall, this zone represents a phase of intensified organic accumulation.

Sedimentary and chemical proxies show interesting associations with the aquatic community. The modern macroinvertebrate community is dominated by Anostraca in Casiri Hembra and by Anostraca, Sarcopiformes, and Diptera in Casiri Macho. Anostraca (Branchiopoda) is an order of crustaceans that generally inhabit ephemeral pools or hypersaline lakes, and they are characteristic of transient (alternately wet and dry), predator-free (e.g., fish) environments (García et al., 2023). In the same way, Sarcopiformes (mites) primarily have carnivorous or parasitic feeding habits, particularly on aquatic insects, and inhabit temporary water bodies—extreme, highly unfavorable environments with very low biological diversity (Proctor and Pritchard, 1989). The occurrence of mite fossil populations in lake sediments can provide clues to the existence of local microhabitats because, unlike many winged insects, mites have lower dispersal ability; therefore, their presence in certain environments indicates that conditions have remained in place that allow them to persist.

Nevertheless, the observed modern structure has not always been the case. Deep sediments from Casiri Macho Lake show a broad dominance of Ostracoda Podocopida in older sediments, alternating with Diptera insects. Ostracods are common in all



types of nonmarine waters with neutral to alkaline pH, and they crawl on or burrow into their substrate, but tend to stay within the shelter of aquatic macrophytes (Holmes, 2002). Mourguiart and Carbonel (1994) showed a clear depth zonation of ostracod species in the large lakes of the Bolivian Altiplano, which they interpreted as reflecting water-depth and lake-level histories. Nevertheless, it seems likely that depth zonation is not a simple response to water depth, but is more linked to the depth distribution of aquatic plants within the lake (Holmes, 1997, 1998). This distribution, therefore, could suggest an indirect response to light availability, as well as to recharge and discharge of surface and groundwater (Holmes, 2002). On the other hand, Diptera insects, especially the most common Chironomids, are heterotrophs that usually feed on algae, fungi, pollen, leaves, detritus, and silt and are therefore expected to be found where organic matter is available. Finally, the observed groups in sediments communities of Casiri Lakes show the attributes proper of population facing harsh environmental conditions, such as wide daily temperature ranges, intense sunlight during the day and very low temperatures at night; strong winds; large variations in oxygen content and pH; large variations in water salinity, being able to adapt to extreme salinities; variations in water level, and seasonal or unexpected drying out or freezing of their habitat. Although these results highlight the macroinvertebrate community's sensitivity to environmental changes in the Caquena basin, a finer contribution to paleoenvironmental reconstruction requires taxonomic identification at the species level for key groups, which is a challenging task for all groups recovered from Casiri lake cores.

Nutrient and mixing gradients are drivers of primary productivity in aquatic ecosystems (Winder and Hunter, 2008). The morphometric characteristics of the lake basin influence the total epilimnion volume and the degree of water-column mixing and thus can be a key factor in lake productivity (Imboden and Wuest, 1995; Wetzel, 2001). The high organic matter may imply a deposition regime dominated by lake productivity. The sedimentation of organic matter plays an important role in the sedimentation of sulfur in oligotrophic lakes; therefore, the observed pattern may reflect the decomposition of organic matter or more reducing water conditions, as observed in the current water column.

Paleoenvironmental studies have been conducted at nearby Chungara Lake (18°14'S, 69°09'W, 4,517 m a.s.l.) situated in the Lauca River basin, 23 km from the Casiri Lakes, but separated from them by the Payachatas range (the Parinacota and Pomerape volcanoes). Results show low water levels during arid phases boosted nutrient recycling and terrestrial organic inputs, increasing organic carbon deposition (Giralt et al., 2008; Moreno et al., 2007; Pueyo et al., 2011; Bao et al., 2015; Jara et al., 2019). Similarly, organic-rich horizons between ~1,202 and ~1,000 yr BP in Casiri Macho may record relatively dry intervals with low lake density and higher organic influx, as evidenced by the increasing percentage of sand. This could indicate a concentration of coarser detritus or more intense runoff. Although organic matter levels rise again in parts of this interval, this increase could be due to episodic algal blooms triggered by doughnuts or terrigenous nutrient pulses. This change in nutrient availability coincides with a significant turnover in community composition. Conversely, the extended wet interval (~2,400-1,600 yr BP) identified in the regional records (Jara et al., 2019) was characterized by higher lake levels, predominantly autochthonous organic matter, and a higher content of fine inputs, such as clays.



This interpretation is further supported by the sedimentological and geochemical characteristics of the sequence, including the
455 dominance of fine-grained fractions and the behavior of detrital elements, which are consistent with a mixed sediment supply
involving both catchment-derived and aeolian inputs (Last and Smol, 2001; Muhs, 2013).

Results obtained from the Chungará Lake sediment records exhibit abrupt millennial-scale fluctuations in water levels that
reflect non-linear responses to global forcing, highlighting the regional sensitivity to changes in atmospheric circulation since
the early Holocene (Giralt et al., 2008; Pueyo et al., 2011; Bao et al., 2015; Orellana et al., 2023). The depositional history of
460 Chungará Lake is dominated by pyroclastic inputs from the sector collapse of Parinacota volcano (~8,000–10,000 yr BP) and
by neotectonic activity along an active normal-fault system (Clavero et al., 2002; Hora et al., 2007; Sáez et al., 2007). This
faulting enhanced sediment supply through bedrock fracturing, leading to high sedimentation rates during the early Holocene
(Sáez et al., 2007). In Casiri lakes, high sedimentation rates were also observed. These high sedimentation rates are difficult
to reconcile solely with fluvial inputs, particularly given the limited hydrological connectivity and the absence of sustained
465 high-energy runoff indicators. This suggests that additional sediment sources must be considered. In this context, sustained
aeolian deposition likely represents a significant contribution to the sediment budget. In arid regions, dust flux can increase
markedly due to enhanced sediment availability and transport efficiency, providing a continuous supply of fine-grained
material to lacustrine systems (Prospero et al., 2002; Mahowald et al., 2010; Muhs, 2013). In such environments, limited
vegetation cover and reduced runoff enhance the availability and mobilization of fine-grained sediments, allowing aeolian
470 processes to act as an efficient transport mechanism into lake basins (Muhs, 2013; Mahowald et al., 2010). Consequently,
sedimentary records from these settings may integrate both catchment-derived and atmospheric signals, particularly under
conditions of increased regional aridity (Prospero et al., 2002). Therefore, the elevated sedimentation rates documented here
may reflect a combination of episodic hydrological inputs and persistent atmospheric deposition. Based on personal
observations, the formation of dunes of varying surface along the southwestern edge of Casiri Hembra Lake during certain
475 periods suggests that wind-driven sediment transport is occurring. Although direct measurements of aeolian flux are
unavailable, the consistency among sedimentological, geochemical, and environmental evidence makes this interpretation
plausible (Last and Smol, 2001).

The local characteristics of this highland basin show several particularities. Geologically, this basin is influenced by volcanic
activity in the Parinacota-Pomerape region and the Kunturiri volcanic complex. Known eruptions (e.g., the Parinacota cone
480 lavas of $\sim 1,660 \pm 350$ yr BP and $\sim 1,400$ yr BP (Wörner et al., 1988, 2000) could have produced records in the core. For
example, the organic-poor layer ~ 59 -60 cm thick ($\sim 1,600$ yr BP) could reflect a volcanic ash deposit that increased the
mineralogical input, and more clearly at ~ 1800 yr BP, where an abrupt increase of feldspars and Fe-Ti oxides were observed,
corresponding a thin layer of volcanic ash/tephra.

Finally, the analysis of Casiri Lakes core offers an opportunity for deepen in further paleoenvironmental and paleoecological
485 studies. Dating and studying the history of different highland water bodies remains a challenge for characterizing the Holocene
climate in the Altiplano. This is due to difficulties in establishing reliable chronological frameworks from the lacustrine
sedimentary infill of most lakes, which requires determining the radiocarbon reservoir effect and its temporal variations (Geyh



and Grosjean, 2000; Hernández et al., 2011). In the case of Casiri Lakes cores, ^{14}C -dated sediments show modern ages for surface sediments, and the date-depth relationship exhibits a linear trend. This, together with the low carbonate content (less than 5%), allows us to infer that, at least up to 3 ky, the reservoir effect is negligible in the Casiri Lakes sediments.

Evidence of volcanic inputs and climatic episodes were observed, in agreement with another Altiplano paleoenvironmental records. Additionally, these results show the relevance of other local drivers, such as an active nutrient recycling that favors greater current productivity and that the nutrient dynamic favor the community turnover. In addition, isolation during arid periods could promote local adaptation in communities from Casiri lakes, as observed in other invertebrates and fish populations (Collado et al., 2011; 2014; Vila et al., 2013), highlighting the microhabitats of the Altiplano as ecological refuges and evolutionary promoters for aquatic populations.

Conclusions

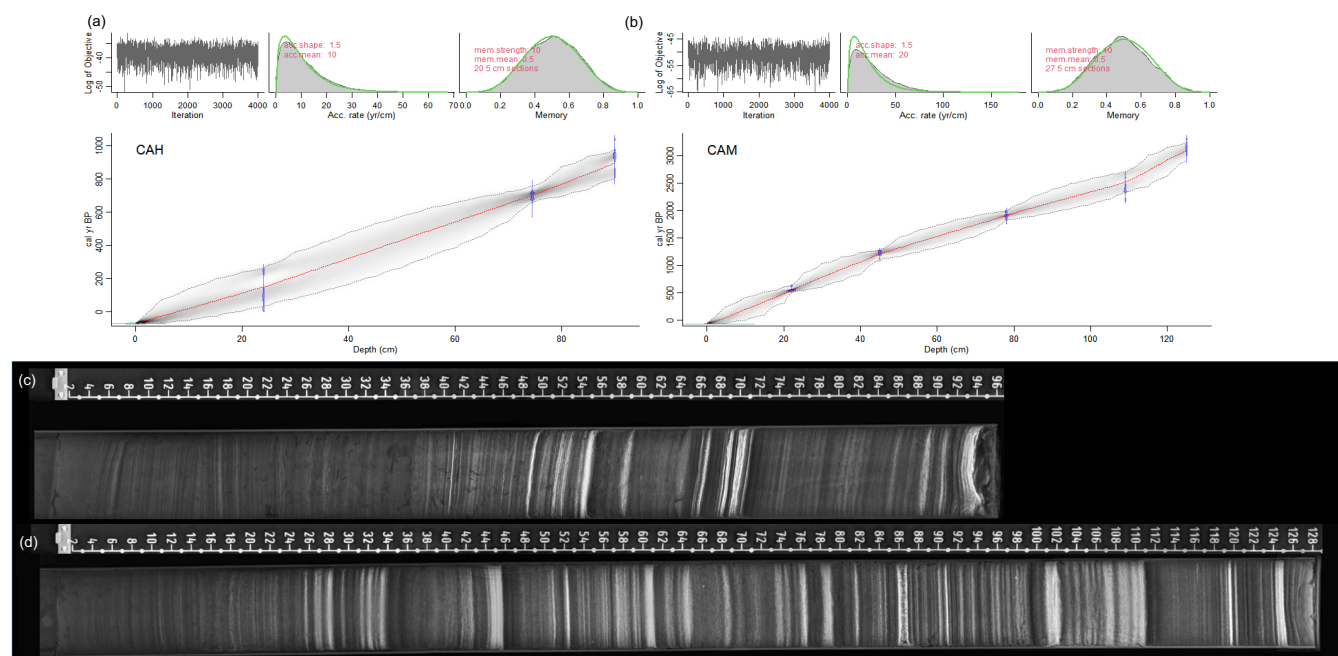
This study provided the first-ever sedimentary cores from two lakes at the northernmost tip of the Chilean Altiplano, at high altitudes $>4,800$ m a.s.l.: Casiri Hembra and Casiri Macho Lakes. Progressive change in depositional dynamics from the Late Holocene to the present were observed, 900 years in Casiri Hembra Lake, and over 3,000 years in Casiri Macho Lake. Older sediments show a general dominance of fine-grained sediments, with episodes reflecting episodic flooding or increased basin runoff, while recent deposits indicate the development of low-energy lacustrine conditions, increased productivity, and/or reduced terrigenous input.

High sedimentation rates were observed suggesting that atmospheric deposition should be considered as a significant contribution to the sediment budget. Also, volcanic activity records have been observed at ~ 1800 yr BP, with a thin layer of volcanic ash/tephra or feldspar-rich debris.

These results show the relevance of an active nutrient recycling in Altiplano lakes that favors greater current productivity and that the nutrient dynamic favor the community turnover.

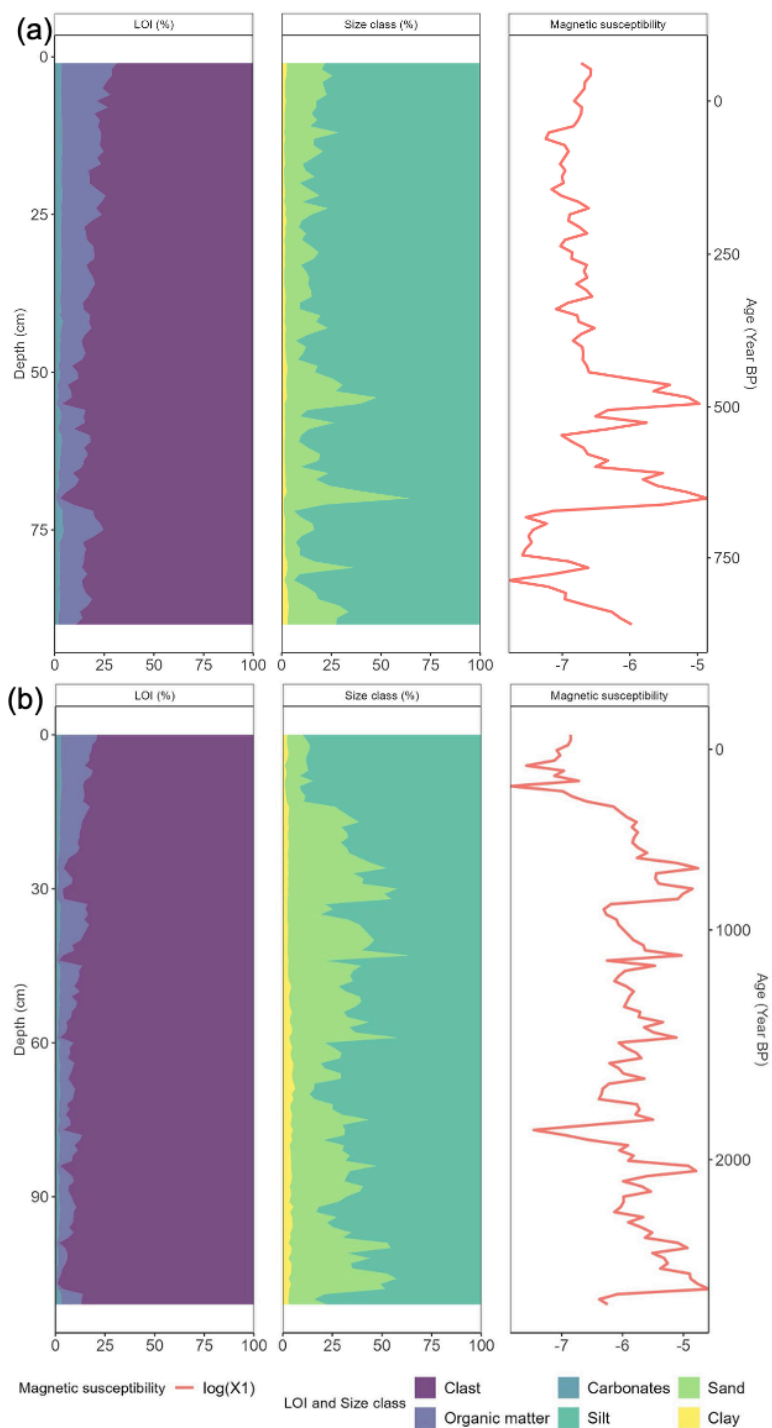


Appendix A



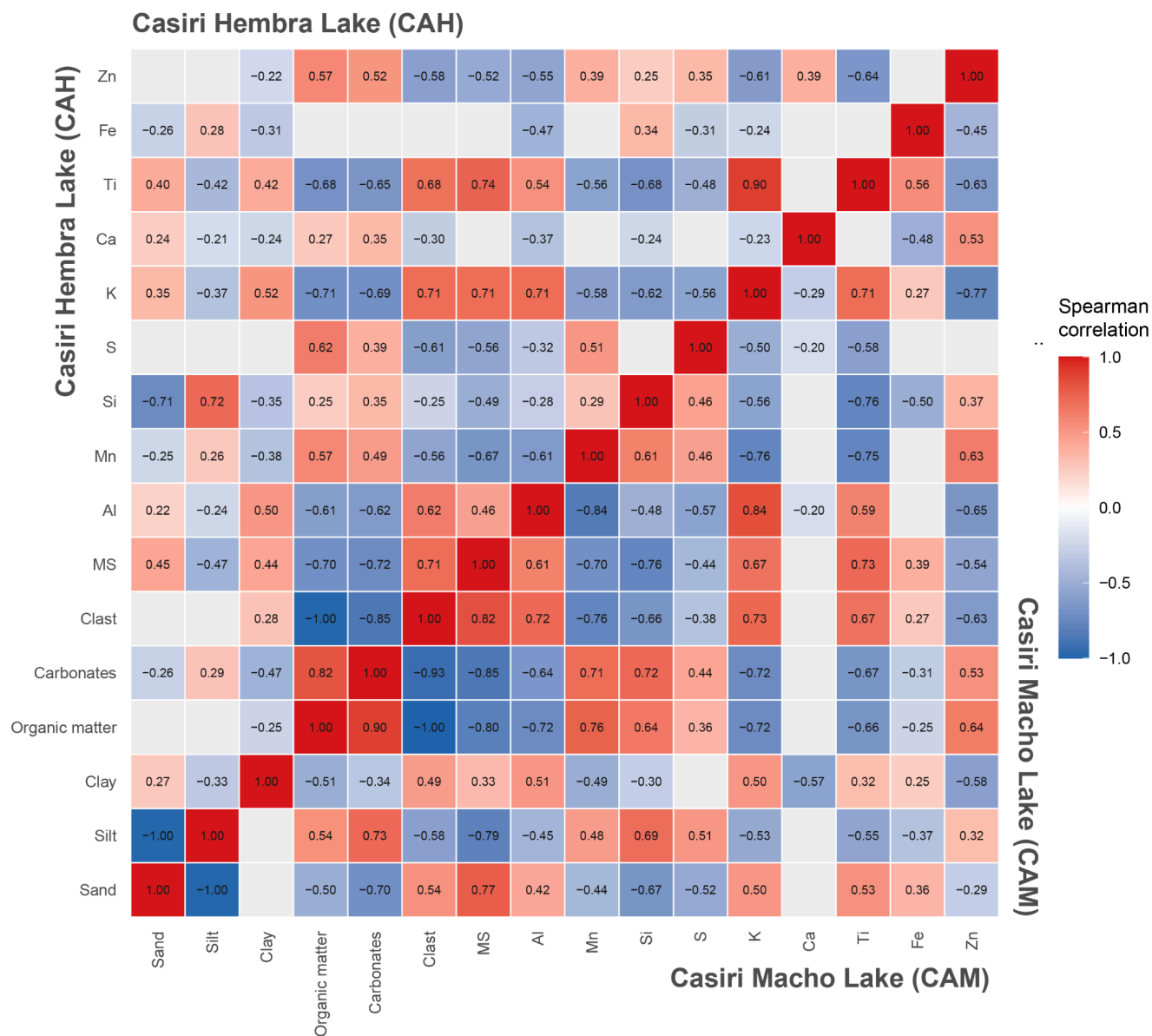
510

Figure A1: Age-depth model for the lacustrine sediment cores from Casiri Hembra Lake (a) and Casiri Macho Lake (b), and X-ray images of CAH-SHC-2 (c), and CAM-SHC-2 (d).



515

Figure A2: Sedimentary analysis plot of loss on ignition (LOI), granulometry (Size class), and magnetic susceptibility (M.S.) for sediment cores from Casiri Hembra (a) and Casiri Macho Lake (b).



520 **Figure A3: Correlation matrix between elemental and sedimentological variables in sediment cores CAH-SHC-2 from Casiri Hembra Lakes and CAM-SHC-2 from Casiri Macho Lake.**

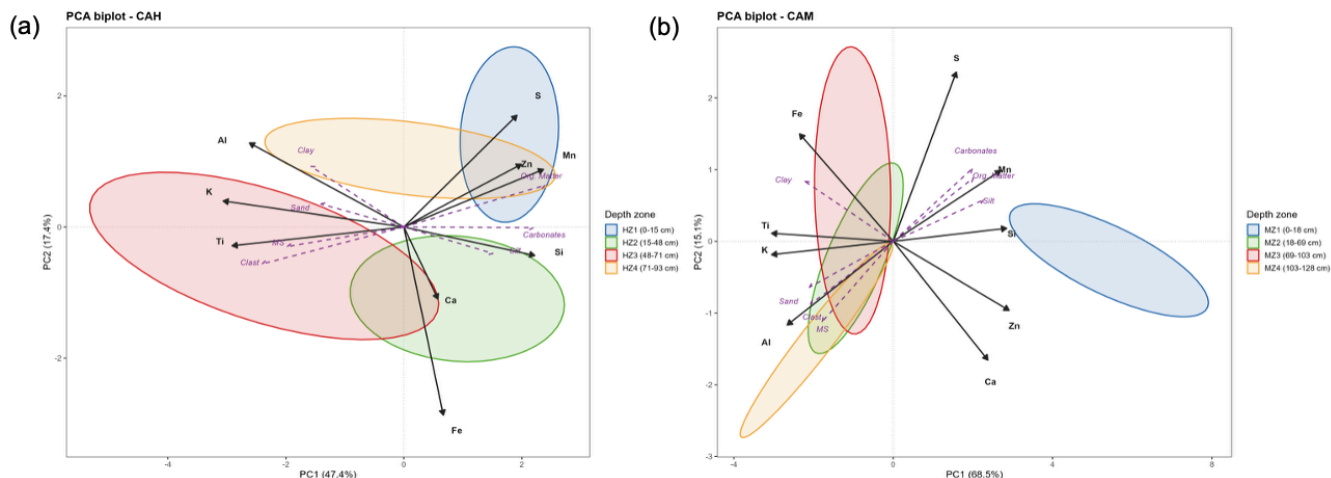


Figure A4. Principal Component Analysis of geochemical and sedimentological variables, clumped by CONISS zones, for cores from Casiri Hembra (a) and Casiri Macho Lake (b).

Code and data availability

525 Raw chemical, magnetic, and ecological data are available in the Zenodo open-access data repository supported by the Conseil Européen pour la Recherche Nucléaire (CERN) (<https://doi.org/10.5281/zenodo.20790045>).

Author contributions

Conceptualization and Funding acquisition: AA-A; Data curation: AA-A, CA, and DP; Fieldwork: AA-A, PP-P, AM, and OM-R; Formal analyses: AA-A, CA, DP, AM, JT, and HP; Writing (original draft preparation): AA-A, CA, DP, and OM-R;
 530 Review and editing: AA-A, DP, CA, JT, AM, HP, PP-P, and OM-R.

Competing interests

The authors declare no conflicts of interest.

Acknowledgements

The authors thank the Mamani-Huanca family from Rinconada de Caquena for their logistical support and for the invaluable
 535 knowledge shared in our conversations. The authors thank to ANID/FONDEQUIP EQM210073 (EULA), and the technical support of Hospital San Juan de Dios, La Serena.



Financial support

This work was supported by ANID-FONDECYT 1200423, UTA-Mayor 9738-24, and ANID–MILENIO–NCS2022_009.

Inclusivity in global research

- 540 This study was conducted in the Aymara territory. Although the aquatic systems studied are not part of Chile’s system of state-protected areas, efforts were made to ensure inclusivity, particularly in the planning and execution of the fieldwork, maximizing the opportunities for in-country partners in all stages of the work.

References

- Acuña-Valenzuela, T., Hernández-Martelo, J., Suazo, M. J., Lobos, I. A., Piñeiro-González, A., Villalobos-Leiva, A., Cruz-
545 Jofré, F., Hernández-P, R., Correa, M., and Benítez, H. A.: Unveiling the Wing Shape Variation in Northern Altiplano Ecosystems: The Example of the Butterfly *Phulia nymphula* Using Geometric Morphometrics, *Animals*, 14(19), 2758, <https://doi.org/10.3390/ani14192758>, 2024.
- Allmendinger, R. W., Jordan, T. E., Kay, S. M., and Isacks, B. L.: The evolution of the Altiplano-Puna plateau of the Central Andes, *Annu. Rev. Earth Planet. Sci.*, 25, 139–174, <https://doi.org/10.1146/annurev.earth.25.1.139>, 1997.
- 550 Ammann, C., Jenny, B., Kammer, K., and Messerli, B.: Late Quaternary Glacier response to humidity changes in the arid Andes of Chile (18–29°S), *Palaeogeogr. Palaeocl.*, 172 (3–4): 313–326. [https://doi.org/10.1016/S0031-0182\(01\)00306-6](https://doi.org/10.1016/S0031-0182(01)00306-6), 2001.
- Baker, P. A., Seltzer, G. O., Fritz, S. C., Dunbar, R. B., Grove, M. J., Tapia, P. M., Cross, S. L., Rowe, H. D., and Broda, J. P.: The history of South American tropical precipitation for the past 25,000 years, *Science*, 291(5504), 640–643,
555 <https://doi.org/10.1126/science.291.5504.640>, 2001.
- Bao, R., Hernández, A., Sáez, A., Giralt, S., Prego, R., Pueyo, J. J., Moreno, A., and Valero-Garcés, B. L.: Climatic and lacustrine morphometric controls of diatom paleoproductivity in a tropical Andean lake, *Quat. Sci. Rev.*, 129, 96–110, <https://doi.org/10.1016/j.quascirev.2015.09.019>, 2015.
- Bengtsson, L. and Enell M.: Chemical analysis, In Berglund, BE (ed.), *Handbook of Holocene Palaeoecology and*
560 *Palaeohydrology*. John Wiley and Sons Ltd., Chichester, UK, 423–451 pp., 1986.
- Bertrand, S., Tjallingii, R., Kylander, M. E., Wilhelm, B., Roberts, S. J., Arnaud, F., Brown, E., and Bindler, R.: Inorganic geochemistry of lake sediments: A review of analytical techniques and guidelines for data interpretation, *Earth-Sci. Rev.*, 249, 104639, <https://doi.org/10.1016/j.earscirev.2023.104639>, 2024.
- Blaauw, M., and Christen, J. A.: Flexible paleoclimate age-depth models using an autoregressive gamma process, *Bayesian*
565 *Anal.*, 6(3), 457–474, <https://doi.org/10.1214/11-BA618>, 2011.



- Catalán, J., Camarero, L., Felip., M., Pla, S., Ventura, M., Buchaca, T., Bartumeus, F., de Mendoza, G., Miró, A., Casamayor, E.O., Medina-Sánchez, J.M., Bacardit, M., Altuna, M., Bartrons, M., and Díaz de Quijano, D.: High mountain lakes: extreme habitats and witnesses of environmental changes, *Limnetica*, 25(1-2), 551-584. <https://doi.org/10.23818/limn.25.38>, 2006.
- Clavero, J.E.: Evolution of Parinacota volcano and Taapaca Volcanic Complex, Central Andes of Northern Chile. Ph.D. Thesis 570 (Unpublished), University of Bristol, 212 p, 2002.
- Clavero, J.E., Sparks, S. J., Polanco V. E., and Pringle, M. S.: Evolution of Parinacota volcano, Central Andes, Northern Chile, *Rev. Geol. Chile*, 31(2), 317-347. <http://dx.doi.org/10.4067/S0716-02082004000200009>, 2004.
- Clavero, J.E., Sparks, S., and Polanco V. E.: Geología del Volcán Parinacota: Región de Arica y Parinacota [versión corregida], Servicio Nacional de Geología y Minería, <https://repositorio.sernageomin.cl/handle/0104/18706>, 2012.
- 575 Clavero, J., Droguett, B., Quiroga, R., and Alvarez, P.: Carta Lago Chungará, Región de Arica y Parinacota, 2018.
- Collado, G. A., Vila, I., and Méndez, M. A.: Monophyly, candidate species and vicariance in *Biomphalaria* snails (Mollusca: Planorbidae) from the Southern Andean Altiplano, *Zool. Scr.*, 40(6), 613–622, <https://doi.org/10.1111/j.1463-6409.2011.00491.x>, 2011.
- Collado, G. A., Salinas, H. F., and Méndez, M. A.: Genetic, morphological, and life history traits variation in freshwater snails 580 from extremely high environments of the Andean Altiplano, *Zool. Stud.*, 53(1), 1–9, <https://doi.org/10.1186/1810-522x-53-14>, 2014.
- De Porras, M.E., Maldonado, A., Hayashida, F.M., Troncoso, A., Salazar, D., Parceros-Oubiña, C., Castro, V., Fábrega-Álvarez, P.: Socio-environmental dynamics in the central Atacama desert (22°S) during the late Holocene, *Quat. Sci. Rev.*, 267(1), 107097, <https://doi.org/10.1016/j.quascirev.2021.107097>, 2021.
- 585 De Silva, S. L.: Styles of zoning in central Andean ignimbrites; Insights into magma chamber processes, *Soc. Am. Spec. Pap.*, 265, 217–232, <https://doi.org/10.1130/SPE265-p217>, 1991.
- Dearing, J. A., Hay, K. L., Baban, S. M. J., Huddleston, A. S., Wellington, E. M. H., and Loveland, P. J.: Magnetic susceptibility of soil: an evaluation of conflicting theories using a national data set, *Geophys. J. Int.*, 127, 728–734, <https://doi.org/10.1111/j.1365-246X.1996.tb04051.x>, 1996.
- 590 Faegri, K. I., and Iversen, J.: Textbook of pollen analysis. Fourth edition. John Wiley and Sons, Chichester, UK, 328 pp., <https://doi.org/10.1002/jqs.3390050310>, 1989.
- García, M., Gardeweg P., M., Clavero R., J., and Hérail, G.: Hoja Arica. Región de Tarapacá. Serie Geología Básica 84, Servicio Nacional de Geología y Minería, Santiago, 2004.
- García, R. D., Jara, F. G. and Abraham, M. S.: New records of fairy shrimp (Anostraca, Branchinectidae) in temporary wetlands 595 from Patagonia, *Pan-Am. J. Aquat. Sci.*, 18(2), 122-126, <https://doi.org/10.54451/PanamJAS.18.2.122>, 2023.
- García-Lino, M. C., Pfanzelt, S., Domic, A. I., Hensen, I., Schitteck, K., Isela Meneses, R., and Bader, M. Y.: Carbon dynamics in high-Andean tropical cushion peatlands: A review of geographic patterns and potential drivers, *Ecol. Monogr.*, 94, e1614, <https://doi.org/10.1002/ecm.1614>, 2023.



- Garzione, C. N., Molnar, P., Libarkin, J. C., and MacFadden, B. J.: Rapid late Miocene rise of the Bolivian Altiplano: Evidence
600 for removal of mantle lithosphere, *Earth Planet. Sci. Lett.*, 241(3–4), 543–556, <https://doi.org/10.1016/J.EPSL.2005.11.026>,
2006.
- Geyh, M., and Grosjean, M.: Establishing a reliable chronology of lake level changes in the Chilean Altiplano: a result of close
collaboration between geochronologists and geomorphologists, *Zbl Geol. Paläont.*, 1, 985–995, 2000.
- Giralt, S., Moreno, A., Bao, R., Sáez, A., Prego, R., Valero-Garcés, B. L., Pueyo, J. J., González-Sampériz, P., and Taberner,
605 C.: A statistical approach to disentangle environmental forcings in a lacustrine record: The lago Chungará case (Chilean
altiplano), *J. Paleolimnol.*, 40, <https://hdl.handle.net/2445/101830>, 2008.
- Grosjean, M., Van Leeuwen, J. F. N., Van Der Knaap, W. O., Geyh, M. A., Ammann, B., Tanner, W., Messerli, B., Núñez, L.
A., Valero-Garcés, B. L., and Veit, H.: A 22,000 14C year BP sediment and pollen record of climate change from Laguna
Miscanti (23°S), northern Chile, *Glob. Planet. Change*, 28(1–4), 35–51, [https://doi.org/10.1016/S0921-8181\(00\)00063-1](https://doi.org/10.1016/S0921-8181(00)00063-1),
610 2001.
- Heiri, O., Lotter, A.F., and Lemcke, G.: Loss on ignition as a method for estimating organic and carbonate content in
sediments: reproducibility and comparability of results, *J. Paleolimnol.*, 25, 101–110,
<https://doi.org/10.1023/A:1008119611481>, 2001.
- Hernández, A., Bao, R., Giralt, S., Barker, P. A., Leng, M. J., Sloane, H. J., and Sáez, A.: Biogeochemical processes controlling
615 oxygen and carbon isotopes of diatom silica in Late Glacial to Holocene lacustrine rhythmites, *Palaeogeogr. Palaeoclimatol.*
Palaeoecol., 412–425, 299 (3–4), <https://doi.org/10.1016/j.palaeo.2010.11.020>. 2011
- Heusser, C.: *Pollen and Spores of Chile: Modern Types of Pteridophyta, Gymnospermae, and Angiospermae*. First edition.
Tucson: University of Arizona, 176 pp., 1971.
- Hodel, F., Macouin, M., Triantafyllou, A., Carlut, J., Berger, J., Rousse, S., Ennih, N., and Trindade, R.I.F.: Unusual massive
620 magnetite veins and highly altered Cr-spinels as relics of a Cl-rich acidic hydrothermal event in Neoproterozoic serpentinites
(Bou Azzer ophiolite, Anti-Atlas, Morocco), *Precambrian Res.*, 300, 151–167,
<https://doi.org/10.1016/j.precamres.2017.08.005>, 2017.
- Hogg, A. G., Heaton, T. J., Hua, Q., Palmer, J. G., Turney, C. S. M., Southon, J., Bayliss, A., Blackwell, P. G., Boswijk, G.,
Ramsey, C. B., Pearson, C., Petchey, F., Reimer, P., Reimer, R., and Wacker, L.: SHCal20 Southern Hemisphere calibration,
625 0–55,000 years cal BP, *Radiocarbon*, 62(4), 759–778, <https://doi.org/10.1017/RDC.2020.59>, 2020.
- Holmes, J. A., Street-Perrott, F. A., Allen, M. J., Fothergill, P. A., Harkness, D. D., Kroon, D., and Perrott, R. A.: Holocene
palaeolimnology of Kajemamm Oasis, Northern Nigeria: an isotopic study of ostracodes, bulk carbonate and organic carbon,
J. Geol. Soc., 154 (2), 311–319, <https://doi.org/10.1144/gsjgs.154.2.0311>, 1997.
- Holmes, J. A., Fothergill, P. A., Street-Perrott, F. A., and Perrott, R. A.: A high-resolution Holocene ostracod record from the
630 Sahel zone of Northeastern Nigeria, *J. Paleolimnol.*, 20, 369–380, <https://doi.org/10.1023/A:1007923304411>, 1998.
- Holmes, J. A. and Chivas, A. R. (Eds.): *Ostracod Shell Chemistry—Overview: The Ostracoda: Applications in Quaternary
Research*, <https://doi.org/10.1029/131GM10>, 2002.



- Hora, J. M., Singer, B. S., and Wörner, G.: Volcano evolution and eruptive flux on the thick crust of the Andean Central Volcanic Zone: $^{40}\text{Ar}/^{39}\text{Ar}$ constraints from Volcán Parinacota, Chile, *Geol. Soc. Am. Bull.*, 119 (3/4), 343–362, <https://doi.org/10.1130/B25954.1>, 2007.
- 635 Imboden, D. M., and Wüest, A.: *Mixing Mechanisms in Lakes*: Lerman, A., Imboden, D. M., Gat, J. R. (eds) *Physics and Chemistry of Lakes*. Springer, Berlin, Heidelberg. https://doi.org/10.1007/978-3-642-85132-2_4, 1995.
- Isacks, B. L.: Uplift of the central Andean Plateau and bending of the Bolivian Orocline, *J. Geophys. Res.*, 93(B4), 3211–3231, <https://doi.org/10.1029/JB093iB04p03211>, 1988.
- 640 Jacobsen, D., and Dangles, O.: *Ecology of High Altitude Waters*, <https://doi.org/10.1093/OSO/9780198736868.001.0001>, 2017.
- Jara, I. A., Maldonado, A., González, L., Hernández, A., Sáez, A., Giralt, S., Bao, R., and Valero-Garcés, B.: Centennial-scale precipitation anomalies in the southern Altiplano (18° S) suggest an extratropical driver for the South American summer monsoon during the late Holocene, *Clim. Past*, 15, 1845–1859, <https://doi.org/10.5194/cp-15-1845-2019>, 2019.
- 645 Jara, I. A., Maldonado, A., and Eugenia de Porras, M.: Late Holocene dynamics of the south American summer monsoon: New insights from the Andes of northern Chile (21°S), *Quat. Sci. Rev.*, 246, 106533, <https://doi.org/10.1016/j.quascirev.2020.106533>, 2020.
- Jordan, T.E., Nester, P.L., Blanco, N., Hoke, G. D., Dávila, F., and Tomlinson, A. J.: Uplift of the Altiplano-Puna plateau: A view from the west, *Tectonics*, 29, TC5007, <https://doi.org/10.1029/2010TC002661>, 2010.
- 650 Juggins, S.: “rioja: Analysis of Quaternary Science Data”, R package version 1.0-7, <https://cran.r-project.org/package=rioja>, 2024.
- Last, W.M., and Smol, J.P. (Eds.): *An Introduction to Physical and Geochemical Methods Used in Paleolimnology*. In: *Tracking Environmental Change Using Lake Sediments. Developments in Paleoenvironmental Research*, vol. 2, Springer, Dordrecht, https://doi.org/10.1007/0-306-47670-3_1, 2001.
- 655 Lee, A.-S., Jyh-Jaan, S. H., Burr, G., Cheng Kao, L., Wei, K.-Y., Liou, H. S.: High resolution record of heavy metals from estuary sediments of Nankan River (Taiwan) assessed by rigorous multivariate statistical analysis, *Quat. Int.*, 527, 44-51, <https://doi.org/10.1016/j.quaint.2018.11.018>, 2019.
- Legendre, P. and Legendre, L.: *Numerical ecology*, *Developments in Environmental Modelling*, 3rd Edition, (Vol. 24), Elsevier, Amsterdam, 419 pp. 2012.
- 660 Lone, A. M. and Balakrishna, K.: Deep and Frozen: High-Mountain Lakes as Sentinels of Regional Limnology and Global Environmental Changes, *Limnol. Oceanogr. Bull.*, 32 (3), 98-101, <https://doi.org/10.1002/lob.10559>, 2023.
- Loria, K. A., Christianson, K. R., and Johnson, P. T.: Phenology of alpine zooplankton populations and the importance of lake ice-out, *J. Plankton Res.*, 42, 727-741, <https://doi.org/10.1093/plankt/fbaa050>, 2020.
- Mahowald, N., Kloster, S., Engelstaedter, S., Moore, J.K., Mukhopadhyay, S., McConnell, Albani S., Doney, S., Bhattacharya, A., Curran, M., Flanner, M., Hoffman, F., Lawrence, D., Lindsay, K., Mayewski, P., Neff, J., Rothenberg, D., Thomas, E.,
- 665



- Thornton, P., Zender, C.: Observed 20th century desert dust variability: impact on climate and biogeochemistry, *Atmos. Chem. Phys.* 10, 10875–10893, <https://doi.org/10.5194/acp-10-10875-2010>, 2010.
- Mahowald, N., Albani, S., Kok, J. F., Engelstaeder, S., Scanza, R., Ward, D. S., and Flanner, M. G.: The size distribution of desert dust aerosols and its impact on the Earth system, *Aeolian Res.*, 15, 53-71, <http://doi.org/10.1016/j.aeolia.2013.09.002>,
670 2014.
- Markgraf, V., and D'Antoni, H.: *Pollen Flora of Argentina, Modern Pollen and Spore Types of Pteridophyta, Gymnospermae, and Angiospermae*, The University of Arizona Press. Arizona, ISBN 0816506493, EE.UU, 1978.
- Mentzer, C., Garziona, C., Jaramillo, C., Hinojosa, L. F., Escobar, J., Glade, N., Gomez, S., Upadhyay, D., Tripathi, A., and Thirumalai, K.: Late Miocene-early Pliocene hydroclimate evolution of the western Altiplano, northern Chile: Implications
675 for aridification trends under warming climate conditions, *Glob. Planet. Change*, 245, 104674, <https://doi.org/10.1016/j.gloplacha.2024.104674>, 2025.
- Metcalf, S. E., Jones, M. D., Davies, S. J., Noren, A., and MacKenzie, A.: Climate variability over the last two millennia in the North American Monsoon region, recorded in laminated lake sediments from Laguna de Juanacatlán, Mexico, *The Holocene*, 28, 1195–1206, <https://doi.org/10.1177/0959683610371994>, 2010.
- 680 Moreno, A., Giralt, S., Valero-Garcés, B., Sáez, A., Bao, R., Prego, R., Pueyo, J.J., González-Sampériz, P., and Taberner, C.: A 14 kyr record of the tropical Andes: The Lago Chungará sequence (18°S, northern Chilean Altiplano), *Quat. Int.*, 161, 4-21, <https://doi.org/10.1016/j.quaint.2006.10.020>, 2007.
- Mottl, O., Grytnes, J. A., Seddon, A. W., Steinbauer, M. J., Bhatta, K. P., Felde, V. A., and Birks, H. J. B.: Rate-of-change analysis in paleoecology revisited: A new approach, *Rev. Palaeobot. Palynol.*, 293, 104483, <https://doi.org/10.1016/j.revpalbo.2021.104483>, 2021.
685
- Mourguiart, P. and Carbonel, P.: A quantitative method of palaeolake-level reconstruction using ostracod assemblages: an example from the Bolivian Altiplano, *Hydrobiologia*, 288, 183–193, <https://doi.org/10.1007/BF00006241>, 1994.
- Muhs, D. R.: The geologic records of dust in the Quaternary, *Aeolian Res.*, 9, 3-48, <https://doi.org/10.1016/j.aeolia.2012.08.001>, 2013.
- 690 Oksanen, J., Blanchet, F. G., Friendly, M., Kindt, R., Legendre, P., McGlinn, D., Minchin, P. R., O'Hara, R. B., Simpson, G. L., Solymos, P., Stevens, M. H. H., Szoecs, E., and Wagner, H.: *vegan: Community Ecology Package*, R package version 2.6-10, <https://CRAN.R-project.org/package=vegan>, 2026.
- Orellana, H., Latorre, C., García, J. L., and Lambert, F.: Spatial analysis of paleoclimate variations based on proxy records in the south-central Andes (18° - 35° S) from 32 to 4 ka, *Quat. Sci. Rev.*, 313, 108174, <https://doi.org/10.1016/j.quascirev.2023.108174>, 2023.
695
- Placzek, C., Quade, J., and Patchett, P. J.: Geochronology and stratigraphy of late Pleistocene lake cycles on the southern Bolivian Altiplano: Implications for causes of tropical climate change, *Geol. Soc. Am. Bull.*, 118(5–6), 515–532, <https://doi.org/10.1130/B25770.1>, 2006.



- 700 Placzek, C., Quade, J., Betancourt, J. L., Patchett, P. J., Rech, J. A., Latorre, C., Matmon, A., Holmgren, C., and English, N.
B.: Climate in the dry central Andes over geologic, millennial, and interannual timescales, *Ann. Mo. Bot. Gard.*, 96(3), 386–
397, <https://doi.org/10.3417/2008019>, 2009.
- Polissar, P. J., Abbott, M. B., Wolfe, A. P., Vuille, M., Bezada, M.: Synchronous interhemispheric Holocene climate trends in
the tropical Andes, *Proc. Natl. Acad. Sci.*, 110(36), 14551–6, <https://doi.org/10.1073/pnas.1219681110>, 2013.
- 705 Proctor, H. C., and Pritchard, G.: Neglected predators: water mites (Acari: Parasitengona: Hydrachnellae) in freshwater
communities, *J. North Am. Benthol. Soc.*, 8(1), 100–111, <https://doi.org/10.2307/1467406>, 1989.
- Prospero, J. M., Ginoux, P., Torres, O., Nicholson, S. E., and Gill, T. E.: Environmental characterization of global sources of
atmospheric soil dust identified with the Nimbus 7 total ozone mapping spectrometer (TOMS) absorbing aerosol product, *Rev.*
Geophys., 40(1), 1002, <https://doi.org/10.1029/2000RG000095>, 2002.
- 710 Pueyo, J. J., Sáez, A., Giralt, S., Valero-Garcés, B. L., Moreno, A., Bao, R., Schwalb, A., Herrera, C., Klosowska, B., and
Taberner, C.: Carbonate and organic matter sedimentation and isotopic signatures in Lake Chungará, Chilean Altiplano, during
the last 12.3 kyr, *Palaeogeogr. Palaeoclimatol. Palaeoecol.*, 307, 339–355, <https://doi.org/10.1016/j.palaeo.2011.05.036>, 2011.
- R Core Team: R: A Language and Environment for Statistical Computing. R Foundation for Statistical Computing, Vienna,
Austria, <https://www.R-project.org/>, 2025.
- 715 Reato, A., Carol, E. S., Cottescu, A., and Martínez, O. A.: Hydrological significance of rock glaciers and other periglacial
landforms as sustenance of wet meadows in Patagonian Andes, *J. South Am. Earth Sci.*, 111, 103471,
<https://doi.org/10.1016/j.jsames.2021.103471>, 2021.
- Sabatier, P., Moernaut, J., Bertrand, S., Van Daele, M., Kremer, K., Chaumillon, E., Arnaud, F.: A review of event deposits in
lake sediments, *Quaternary*, 5, 34, <https://doi.org/10.3390/quat5030034>, 2022.
- 720 Sáez, A., Valero-Garcés, B. L., Moreno, A., Bao, R., Pueyo, J. J., González-Sampériz, P., Giralt, S., Taberner, C., Herrera, C.,
and Gibert, R. O.: Lacustrine sedimentation in active volcanic settings: The Late Quaternary depositional evolution of Lake
Chungará (northern Chile), *Sedimentology*, 54(5), 1191–1222, <https://doi.org/10.1111/j.1365-3091.2007.00878.x>, 2007.
- Schwestermann, T., Huang, J., Konzett, J., Kioka, A., Wefer, G., Ikehara, K., Moernaut, J., Eglinton, T.I., and Strasser, M.:
Multivariate statistical and multiproxy constraints on earthquake-triggered sediment remobilization processes in the central
Japan Trench, *Geochem. Geophys. Geosyst.*, 21, e2019GC008861. <https://doi.org/10.1029/2019GC008861>, 2020.
- 725 Stern, C. R.: Active andean volcanism: its geologic and tectonic setting, *Rev. geol. Chile*, 31(2), 161–206,
<http://doi.org/10.4067/S0716-02082004000200001>, 2004.
- Stockmarr, J. Tablets with Spores Used in Absolute Pollen Analysis. *Pollen et Spores*, 13, 615–621, 1971.
- 730 Tapia, P. M., Fritz, S. C., Baker, P.A., Seltzer, G. O., and Dunbar, R. B.: A Late Quaternary diatom record of tropical climatic
history from Lake Titicaca (Peru and Bolivia), *Palaeogeogr. Palaeoclimatol. Palaeoecol.*, 194(1–3), 139–164,
[https://doi.org/10.1016/S0031-0182\(03\)00275-X](https://doi.org/10.1016/S0031-0182(03)00275-X), 2003.



- Tapia, J., Audry, S., Townley, B., and Duprey, J. L.: Geochemical background, baseline and origin of contaminants from sediments in the mining-impacted Altiplano and Eastern Cordillera of Oruro, Bolivia, *Geochem. Explor. Environ. Anal.*, 12(1), 3–20, <https://doi.org/10.1144/1467-7873/10-RA-049>, 2012.
- Tapia, J., Murray, J., Ormachea, M., Tirado, N., and Nordstrom, D. K.: Origin, distribution, and geochemistry of arsenic in the
735 Altiplano-Puna plateau of Argentina, Bolivia, Chile, and Perú, *Sci. Total Environ.*, 678, 309–325, <https://doi.org/10.1016/j.scitotenv.2019.04.084>, 2019.
- Telford, R. J., Barker, P., Metcalfe, S., and Newton, A.: Lacustrine responses to tephra deposition: examples from Mexico, *Quat. Sci. Rev.*, 23(23–24), 2337–2353, <https://doi.org/10.1016/j.quascirev.2004.03.014>, 2004.
- Tucker, M. E.: *Sedimentary Petrology: An Introduction to the Origin of Sedimentary Rocks*. Hoboken, NJ: Blackwell Science
740 Ltd, 11–65, 2009.
- Valero-Garcés, B. L., Grosjean, M., Kelts, K., Schreier, H., and Messerli, B.: Holocene lacustrine deposition in the Atacama Altiplano: facies models, climate and tectonic forcing, *Palaeogeogr. Palaeoclimatol. Palaeoecol.*, 151(1–3), 101–125, [https://doi.org/10.1016/S0031-0182\(99\)00018-8](https://doi.org/10.1016/S0031-0182(99)00018-8), 1999.
- Vila, I., Morales, P., Scott, S., Poulin, E., Véliz, D., Harrod, C., and Méndez, M. A.: Phylogenetic and phylogeographic analysis
745 of the genus *Orestias* (Teleostei: Cyprinodontidae) in the southern Chilean Altiplano: The relevance of ancient and recent divergence processes in speciation, *J. Fish Biol.*, 82(3), 927–943, <https://doi.org/10.1111/jfb.12031>, 2013.
- Villagrán, C. *Vegetationsgeschichtliche und pflanzensoziologische Untersuchungen im Vicente-Pérez-Rosales-Nationalpark (Chile)*. *Dissertationes Botanicae*, Band, Vol. 54, Gettingen, Deutschland, 1980.
- Weltje, G. J., Bloemsa, M. R., Tjallingii, R., Heslop, D., Röhl, U., and Croudace, I. W.: Prediction of geochemical
750 composition from XRF core scanner data: A new multivariate approach including automatic selection of calibration samples and quantification of uncertainties. In *Micro-XRF studies of sediment cores: Applications of a non-destructive tool for the environmental sciences* (pp. 507–534). Springer Netherlands, https://doi.org/10.1007/978-94-017-9849-5_21, 2015.
- Wetzel, R.G.: *Limnology: Lake and River Ecosystems*, Third Edition, Academic Press. San Francisco, 429 pp, <https://doi.org/10.1016/C2009-0-02112-6>, 2001.
- 755 Winder, M., and Hunter, D. A.: Temporal organization of phytoplankton communities linked to physical forcing, *Oecologia*, 156(1), 179–192, <https://doi.org/10.1007/s00442-008-0964-7>, 2008.
- Wörner, G., Harmon, R., Davidson, J., Moorbath, S., Turner, D., McMillan, N., Nye, C., López, L., and Moreno, H.: The Nevados de Payachata volcanic region (18°S/69°W, N. Chile) I. Geological, geochemical and isotopic observations, *Bull. Volcanol.*, 50, 287–303, <https://doi.org/10.1007/BF00286829>, 1988.
- 760 Wörner, G., Hammerschmidt, K., Henjes-Kunst, F., Lezaun, J., and Wilke, H.: Geochronology (⁴⁰Ar/³⁹Ar, K-Ar and He-exposure ages) of Cenozoic magmatic rocks from northern Chile (18–22°S): implications for magmatism and tectonic evolution of the central Andes, *Rev. Geol. Chile*, 27(2), 205–240, <http://dx.doi.org/10.4067/S0716-02082000000200004>, 2000.